AMERICAN SOCIETY FOR MICROBIOLOGY | Infection and Immunity

Control of *Clostridium difficile* Physiopathology in Response to Cysteine Availability

Thomas Dubois,[a] Marie Dancer-Thibonnier,[a] Marc Monot,[a] Audrey Hamiot,[a] Laurent Bouillaut,[c]* Olga Soutourina,[a,b] Isabelle Martin-Verstraete,[a,b] Bruno Dupuy[a]

Laboratoire Pathogenèse des Bactéries Anaérobies, Institut Pasteur, Paris, France[a]; Université Paris 7-Denis Diderot, Paris, France[b]; Department of Molecular Biology and Microbiology, Tufts University School of Medicine, Boston, Massachusetts, USA[c]

The pathogenicity of *Clostridium difficile* is linked to its ability to produce two toxins: TcdA and TcdB. The level of toxin synthesis is influenced by environmental signals, such as phosphotransferase system (PTS) sugars, biotin, and amino acids, especially cysteine. To understand the molecular mechanisms of cysteine-dependent repression of toxin production, we reconstructed the sulfur metabolism pathways of *C. difficile* strain 630 *in silico* and validated some of them by testing *C. difficile* growth in the presence of various sulfur sources. High levels of sulfide and pyruvate were produced in the presence of 10 mM cysteine, indicating that cysteine is actively catabolized by cysteine desulfhydrases. Using a transcriptomic approach, we analyzed cysteine-dependent control of gene expression and showed that cysteine modulates the expression of genes involved in cysteine metabolism, amino acid biosynthesis, fermentation, energy metabolism, iron acquisition, and the stress response. Additionally, a sigma factor (SigL) and global regulators (CcpA, CodY, and Fur) were tested to elucidate their roles in the cysteine-dependent regulation of toxin production. Among these regulators, only *sigL* inactivation resulted in the derepression of toxin gene expression in the presence of cysteine. Interestingly, the *sigL* mutant produced less pyruvate and H_2S than the wild-type strain. Unlike cysteine, the addition of 10 mM pyruvate to the medium for a short time during the growth of the wild-type and *sigL* mutant strains reduced expression of the toxin genes, indicating that cysteine-dependent repression of toxin production is mainly due to the accumulation of cysteine by-products during growth. Finally, we showed that the effect of pyruvate on toxin gene expression is mediated at least in part by the two-component system CD2602-CD2601.

Clostridium difficile is a Gram-positive spore-forming obligate anaerobe and the major cause of nosocomial diarrhea associated with antibiotic therapy. The symptoms of *C. difficile* infection (CDI) vary from mild diarrhea to life-threatening pseudomembranous colitis, a severe form of CDI (1). Virulent *C. difficile* strains produce two large toxins: an enterotoxin (TcdA) and a cytotoxin (TcdB). The *tcdA* and *tcdB* genes are clustered within a single chromosomal region, called the pathogenicity locus (PaLoc), with three accessory genes: *tcdR*, *tcdE*, and *tcdC*. The expression of the toxin genes is controlled through the coordinated action of the alternative sigma factor TcdR and its antagonist factor, TcdC (2–4). The *tcdE* gene encodes a holin-like protein that is required for toxin release (5).

The spectrum of diseases caused by *C. difficile* depends on host factors and, for the severe forms, on the level of toxins produced, suggesting that the regulation of toxin synthesis is a critical determinant of *C. difficile* pathogenicity (6). Toxin production starts when *C. difficile* cultures enter the stationary growth phase (7) and is modulated in response to various environmental signals. Exposure to subinhibitory concentrations of antibiotics, a temperature of 37°C, biotin limitation, or the presence of butyric acid stimulates toxin production (8, 9). In contrast, the presence of rapidly metabolized carbon sources, such as glucose and butanol, or amino acids, such as cysteine and proline, inhibits toxin synthesis (7, 10–12). Some of the molecular mechanisms regulating *C. difficile* toxin synthesis in response to environmental signals have been elucidated (13–16). It has been shown that CodY, the global regulator involved in the adaptive response to nutrient limitation, represses toxin gene expression by binding to the *tcdR* promoter region (14, 17) and that glucose-dependent repression of toxin production is mediated by CcpA, the global regulator of carbon catabolite repression (CCR) (13). This repression is the result of the direct binding of CcpA to a *cis*-acting catabolite response element (*cre* site) that is present in the regulatory regions of the *tcdA*, *tcdB*, *tcdR*, and *tcdC* genes, with the strongest affinity observed for the *tcdR* promoter (18). Toxin gene expression also depends on transcriptional factors, such as SigH and Spo0A, which control the transition to the postexponential growth phase and the initiation of sporulation (15, 16).

Changes in colonic flora after antibiotic treatment lead to the modification of metabolic pools, which affects the spore germination and cell growth of *C. difficile* (19). Specifically, the levels of several phosphotransferase system (PTS) sugars, such as mannitol and sorbitol, and amino acids, such as proline, cysteine, and cystine, the cysteine dimer, increase during gut dysbiosis. These compounds are metabolized by *C. difficile* and may serve as metabolic

Received 10 February 2016 **Returned for modification** 25 February 2016
Accepted 31 May 2016

Accepted manuscript posted online 13 June 2016

Citation Dubois T, Dancer-Thibonnier M, Monot M, Hamiot A, Bouillaut L, Soutourina O, Martin-Verstraete I, Dupuy B. 2016. Control of *Clostridium difficile* physiopathology in response to cysteine availability. Infect Immun 84:2389–2405. doi:10.1128/IAI.00121-16.

Editor: V. B. Young, University of Michigan

Address correspondence to Bruno Dupuy, bdupuy@pasteur.fr.

* Present address: Laurent Bouillaut, Matrivax R&D, Boston, Massachusetts, USA.

T.D., M.D.-T., I.M.-V., and B.D. contributed equally to this article.

Supplemental material for this article may be found at http://dx.doi.org/10.1128/IAI.00121-16.

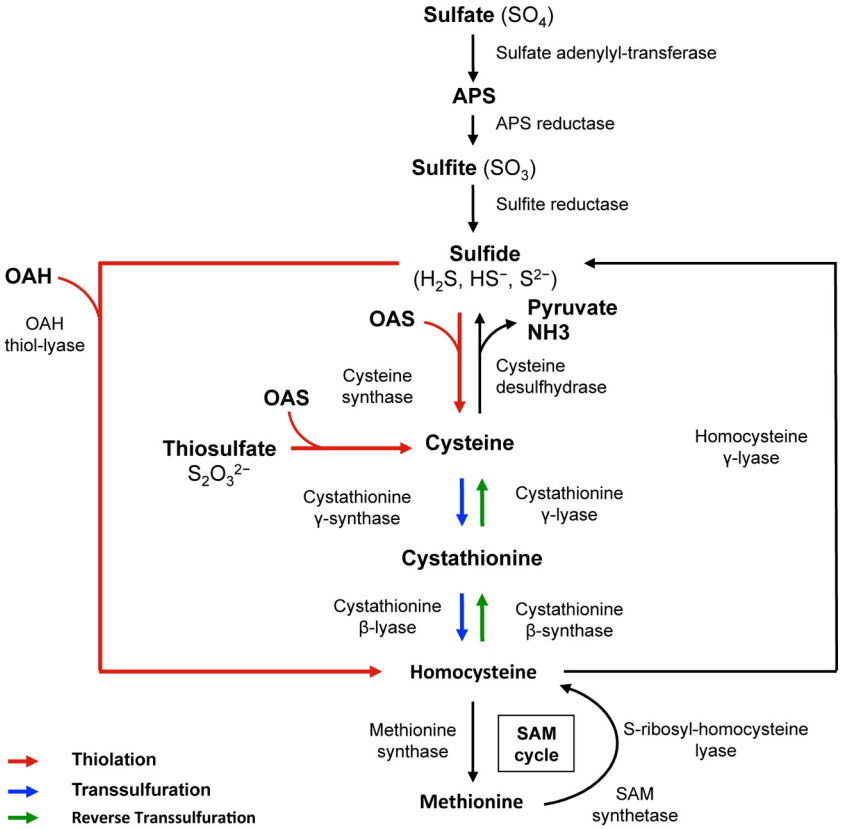

FIG 1 Schematic overview of sulfur metabolism in bacteria. APS, adenylyl sulfate; OAS, *O*-acetylserine; OAH, *O*-acetylhomoserine; SAM, *S*-adenosyl-methionine.

signals that are detected by regulators to coordinate adaptation, growth, and virulence factor production during gut colonization.

Among the amino acids that downregulate toxin production in *C. difficile* strains, cysteine is the most potent (11, 12). Links between bacterial virulence and cysteine metabolism have been described in several pathogenic bacteria. In *Clostridium perfringens* and *Bordetella pertussis*, toxin synthesis is regulated in response to cysteine availability (20, 21). Additionally, genes involved in sulfur metabolism are induced when *Mycobacterium tuberculosis*, *Yersinia ruckeri*, *Staphylococcus aureus*, and *Nesseiria meningitidis* interact with human cells (22–24). In addition, loss-of-function mutations in genes involved in cysteine biosynthesis or degradation affect the virulence for some of these pathogens (23–26). Finally, the master regulator of cysteine metabolism in *S. aureus*, CymR, plays an important role in both the stress response and the control of bacterial virulence (27).

The sulfur-containing amino acid cysteine is central to bacterial physiology. This amino acid is a precursor of methionine and of several coenzymes (biotin, thiamine, coenzyme A [CoA], and coenzyme M). Cysteine is also the sulfur donor for the biogenesis of the iron-sulfur (Fe-S) clusters that are found in the catalytic site of several enzymes and assists in protein folding and assembly by forming disulfide bonds. Moreover, cysteine-containing proteins (thioredoxin and glutaredoxin) and molecules (glutathione, bacillithiol, and mycothiol) are important in protecting cells against oxidative stress (28, 29). Two major cysteine biosynthetic pathways are present in microorganisms: (i) the thiolation pathway, which directly incorporates sulfide or thiosulfate into *O*-acetyl L-serine (OAS), and (ii) the reverse transsulfuration pathway, which converts homocysteine into cysteine via a cystathionine intermediate (Fig. 1) (30, 31). Homocysteine is synthesized from methionine using the *S*-adenosyl-methionine (SAM) recycling pathway, while sulfide arises mostly from the reduction of sulfate.

Due to the reactivity of its thiol group, the intracellular concentration of cysteine must be tightly controlled. The pathways responsible for depleting free cysteine include those that incorporate cysteine into molecules (proteins, methionine, Fe-S clusters, and vitamins) and those that degrade or export it (30). Cysteine can also be catabolized by cysteine desulfhydrases or cysteine desulfidase, producing pyruvate and hydrogen sulfide (H_2S) (Fig. 1) (24, 32). Finally, a large variety of molecular mechanisms participate in fine-tuning cysteine metabolism in response to environmental changes. These systems include regulation by the premature termination of transcription at T-box systems in response to the level of charge of $tRNA_{Cys}$ (33) or by several transcriptional regulators, including activators of the LysR family (30) and CymR, a repressor of the Rrf2 family (34, 35).

To understand the molecular mechanisms involved in the cysteine response, we performed a reconstruction of *C. difficile* sulfur metabolism and analyzed the global effect of cysteine on gene expression. Then, we showed that cysteine-dependent repression of toxin production requires SigL. Moreover, we observed that the production of pyruvate and H_2S decreased in the *sigL* mutant compared to that in the wild-type strain. Interestingly, addition of

TABLE 1 Strains and plasmids used in this study

Strain or plasmid	Characteristic	Gene type	Plasmid or resistance type[a]	Origin or reference
Strains	Background	Knockout or overexpressed gene	Plasmid	
630Δ*erm*				87
M7404	BI/NAP1/027			2
M7404 (*tcdC*$^+$)	BI/NAP1/027		pDLL17 (*tcdC*$^+$)	2
VPI 10463				Virginia Polytechnic Institute
CDIP001	630Δ*erm*	*CD1287* (*fur*)::*erm*		This study
CDIP106	630Δ*erm*	*CD0278*::*erm*		This study
CDIP107	630Δ*erm*	*CD2023*::*erm*		This study
CDIP110	630Δ*erm*	*CD2065*::*erm*		This study
CDIP217	630Δ*erm*	*CD3176* (*sigL*)::*erm*		This study
CDIP342	630Δ*erm*	*CD3176* (*sigL*)::*erm*	pDIA6309	This study
CDIP540	630Δ*erm*	*CD1594* (*cysK*)::*erm*		This study
CDIP656	630Δ*erm*		pDIA6456	This study
CDIP657	630Δ*erm*	*CD2602*::*erm*		This study
JIR8094				88
CDIP100	JIR8094	*CD1064* (*ccpA*)::*erm*		13
LB-CD15	JIR8094	*CD1275* (*codY*)::*erm*	pBL92	L. Bouillaut
Plasmids	Vector	Cloned gene	Resistance	Origin
pDIA5906	pMTL007	Intron *CD1287* (*fur*)	Cm^r Tm^r	This study
pDIA6309	pMTL84121	*CD3176* (*sigL*)	Cm^r Tm^r	This study
pDIA6450	pMTL007	Intron *CD0278*	Cm^r Tm^r	This study
pDIA6451	pMTL007	Intron *CD2065*	Cm^r Tm^r	This study
pDIA6452	pMTL007	Intron *CD2023*	Cm^r Tm^r	This study
pDIA6453	pMTL007	Intron *CD3176*	Cm^r Tm^r	This study
pDIA6454	pMTL007	Intron *CD2602*	Cm^r Tm^r	This study
pDIA6455	pMTL007	Intron *CD1594* (*cysK*)	Cm^r Tm^r	This study
pDIA6456	pRPF185	Antisense *CD3029* (*malY*)	Cm^r Tm^r	This study

[a] Cm, chloramphenicol; Tm, thiamphenicol; Erm, erythromycin.

pyruvate to the growth medium of the wild-type and the *sigL* mutant strains repressed toxin gene transcription, suggesting that the effect of cysteine on toxin production is due, at least in part, to the accumulation of cysteine by-products resulting from cysteine degradation. Finally, we showed that the regulation of toxins by exogenous pyruvate is mediated by a two-component system (TCS) through a still uncharacterized mechanism.

MATERIALS AND METHODS

Bacterial strains and culture conditions. The *C. difficile* strains used in this study are described in Table 1. *Escherichia coli* strain NEB 10-beta (BioLabs) and *E. coli* strain HB101(RP4) were used, respectively, for cloning and as a donor strain for *C. difficile* conjugation experiments. *C. difficile* strains were grown anaerobically (5% H_2, 5% CO_2, 90% N_2) in PY medium (20 g/liter Bacto peptone, 10 g/liter yeast extract, 0.4% [2 ml/liter] $CaCl_2$, 0.025% [4 ml/liter] resazurin, 0.05% [10 ml/liter] hemin, 0.05% [1 ml/liter] vitamin K, and 40 ml/liter of salts solution containing 1 g/liter K_2HPO_4, 1 g/liter KH_2PO_4, 10 g/liter $NaHCO_2$, 2 g/liter NaCl, and 0.2 g/liter $MgSO_4 \cdot 7H_2O$), PYC (PY with 10 mM cysteine), or PYHC medium (PY with 10 mM homocysteine) (12). After 9 h of cell growth, 15 mM acetate or 10 mM pyruvate, Na_2S, or formate was added to the PY medium. When necessary, cefoxitin (25 μg/ml), thiamphenicol (15 μg/ml), or erythromycin (2.5 μg/ml) was added to *C. difficile* cultures. *E. coli* strains were grown in Luria-Bertani (LB) broth. When indicated, ampicillin (100 μg/ml) or chloramphenicol (15 μg/ml) was added to the culture medium. Additionally, 200 ng/ml of anhydrotetracycline (Atc) was used to induce the P_{tet} promoter of the pRPF185 vector derivatives in *C. difficile* (36). The sulfur-free minimal medium was as previously described (20), with the addition of 0.3 g/liter of proline. The concentrations of the sulfur sources added are indicated in Table 2.

Dot blot analysis. Crude extracts were obtained using the FastPrep (MP Biomedicals) cell lysis system (speed, 6; time, 40 s; performed twice), followed by centrifugation (10 min at 4°C) to remove cell debris. For dot blot experiments, 20 ng (VPI 10463) or 200 ng (630Δ*erm*, M7404, and M7404 *tcdC*$^+$ strains) of proteins from the crude extracts was directly spotted onto a nitrocellulose membrane (Hybond-C Extra; Amersham Biosciences). The membranes were blocked with 5% (wt/vol) nonfat dried milk in Tris-buffered saline (TBS) supplemented with 0.2% (vol/vol) Tween 20 (TBST) for 1 h at room temperature. The membranes were then incubated for 90 min at 37°C with the TcdA antibody (PCG-4; Santa Cruz Biotechnology) and visualized as described by Antunes et al. (13).

Cell cultures and cytotoxicity assays. Vero cells were cultured in Dulbecco's modified Eagle's medium (DMEM [Gibco]) supplemented with

TABLE 2 Growth of *C. difficile* strain 630Δ*erm* in minimal medium containing different sulfur sources

Sulfur source (concn)	Growth at[a]: 16 h	48 h
Sulfate (4 mM)	−	−
Sulfite (4 mM)	−	−
Sulfide (4 mM)	+	+
Thiosulfate (4 mM)	−	+
Cysteine (4 mM)	+	+
Cystine (2 mM)	−	+
Glutathione (2 mM)	+	+
Cystathionine (2 mM)	−	+
Homocysteine (2 mM)	+	+
Methionine (1.5 mM)	−	−

[a] +, growth; −, no growth.

5% (vol/vol) fetal calf serum and a 1% ready-to-use solution (vol/vol) of penicillin (10,000 U ml^{-1}) and streptomycin (10 mg ml^{-1}) (Sigma) at 37°C in a 5% CO_2 atmosphere. For cytotoxicity assays, cells were grown until confluence in 96-well plates and incubated with 2-fold serially diluted *C. difficile* crude extracts in DMEM. After 24 h at 37°C, the cytopathic effect was evaluated using an optical microscope. Positive toxin reactions were indicated by the characteristic rounding of Vero cells. The titer of each sample corresponds to the well containing 50% round Vero cells.

Detection and quantification of hydrogen sulfide and pyruvate production. H_2S production was detected using lead-acetate paper (Macherey-Nagel), which turns black in the presence of this compound. Cells were grown in PY, PYC, or PYHC to an optical density at 600 nm (OD_{600}) of 0.7. Then, the lead-acetate paper was placed at the bottom of the flask for 1 min to 1 h at 37°C, depending on the experiment. H_2S production was further quantified as previously described (31, 37). Briefly, 5 ml of the 630Δ*erm* strain culture was introduced into a flask with an alkaline agar layer enriched with zinc acetate and incubated for 1 h at 37°C. The OD_{670} was measured against an H_2O blank. The amount of H_2S was calculated using a standard curve of Na_2S. For pyruvate quantification, cells were grown in PY or PYC for 10 h at 37°C, and pyruvate was quantified in the supernatant using a Sigma pyruvate assay kit. The final pyruvate concentration was standardized using the OD_{600} of the bacterial cultures.

Estimation of the intracellular amino acid content. The intracellular concentrations of amino acids were estimated using high-pressure liquid chromatography (HPLC) (31, 38). Briefly, cells were suspended in a sulfosalicylic acid buffer (3% final concentration) and disrupted using a Fastprep apparatus (MP Biomedicals). After centrifugation, supernatant samples were analyzed by cation-exchange chromatography, followed by ninhydrin postcolumn derivatization as previously described (31).

Zymogram. Zymograms were used to detect the cysteine desulfhydrase and homocysteine γ-lyase activities. Native protein crude extracts (40 and 100 μg, respectively) were run on a nondenaturing protein gel (12% polyacrylamide in Tris-glycine buffer). After electrophoresis, the gel was incubated at 37°C for 1 to 4 h in a Tris solution [50 mM Tris-HCl (pH 7.4), 10 mM $MgCl_2$, 0.5 mM $Pb(NO_3)_2$, and 5 mM dithiothreitol (DTT)] with 0.4 mM pyridoxal-5-phosphate (PLP) containing either 10 mM L-cysteine or 10 mM homocysteine as previously described (32). H_2S formed by the cysteine desulfhydrase or homocysteine γ-lyase activity precipitates as insoluble PbS.

Construction of *C. difficile* mutants. The ClosTron gene knockout system (39) was used to inactivate genes encoding Fur (*CD1287*), SigL (*CD3176*), CysK (*CD1594*), and a TCS sensor histidine kinase (*CD2602*), as well as several regulators of unknown function (*CD2065*, *CD0278*, and *CD2023* [Table 1]). As described in Fig. S1 in the supplemental material, primers were designed to retarget the group II intron of pMTL007 to these genes (see Table S1 in the supplemental material) and were used to generate a 353-bp DNA fragment by overlap PCR according to the manufacturer's instructions. These PCR products were cloned into the HindIII and BsrGI restriction sites of pMTL007 and were verified by DNA sequencing using the pMTL007-F and pMTL007-R primers (see Table S1). The derived pMTL007 plasmids were transformed into *E. coli* strain HB101(RP4) and transferred by conjugation into the *C. difficile* strain 630Δ*erm*. *C. difficile* transconjugants were selected by subculture on brain heart infusion (BHI) agar containing thiamphenicol (15 μg/ml), and the integration of the group II intron RNA into genes was induced and selected by plating onto BHI agar containing erythromycin (2.5 μg/ml). The chromosomal DNA of the transconjugants was extracted using the InstaGene kit (Bio-Rad), and PCR with the primers ErmRAM-F and ErmRAM-R (see Table S1) was used to confirm the erythromycin-resistant phenotype due to the splicing of the group I intron from the group II intron following integration (see Fig. S1A). The insertion of the group II intron into target genes was verified by Southern blotting (see Fig. S1C) and by PCRs (see Fig. S1B) with primers flanking the 5′ ends of genes (see Table S1) and EBSu primer. To knock down *malY* (*CD3029*) expression, a DNA fragment comprising the 5′ untranslated region (UTR) and the beginning of the *CD3029* open reading frame (−38 to +154 from the ATG start codon) was amplified by PCR and cloned between the XhoI and BamHI sites of the pRPF185 vector (36) to generate pDIA6456 expressing the 5′ end of *malY* in the antisense orientation under the control of the ATc-inducible P_{tet} promoter. This plasmid was transferred by conjugation into *C. difficile* strain 630Δ*erm*. To complement the *sigL* mutant, the *sigL* gene and its promoter (−193 to +1380 from the ATG start codon) were amplified by PCR using the appropriate primers (see Table S1). The PCR fragment was cloned into the XhoI and BamHI sites of pMTL84121 (40) to generate plasmid pDIA6309. This plasmid was transferred by conjugation into the *C. difficile sigL* mutant (CDIP217), yielding strain CDIP342.

All experiments conducted with the mutants were standardized versus the wild type for the culture growth (OD_{600}) and the protein concentration of the samples or by using a reference gene for the quantitative reverse transcriptase PCR (qRT-PCR) assays.

RNA isolation and quantitative real-time PCR. *C. difficile* strains were grown in PY or PYC for 10 h. Total RNA extraction was performed using the FastRNA Pro Blue kit and a FastPrep apparatus according to the manufacturer's instructions (MP Biomedicals) as previously described (13). To synthesize cDNA, 1 μg of total RNA was heated at 70°C for 10 min in the presence of 1 μg of hexamer oligonucleotide primers (pdN_6; Roche). RNAs were then reverse transcribed for 2 h at 37°C using an avian myeloblastosis virus (AMV) reverse transcriptase (RT) (Promega), 20 mM deoxynucleoside triphosphates (dNTPs), and 40 U of RNasin (Promega). Reverse transcriptase was inactivated by heating at 85°C for 5 min. Real-time quantitative RT-PCR was performed in a 20-μl reaction volume containing 20 ng of cDNAs, FastStart SYBR green master mix (ROX; Roche), and 200 nM gene-specific primers (see Table S1 in the supplemental material). Amplification and detection were performed as previously described (13). The quantity of each cDNA was normalized to the quantity of the cDNA of the DNA polymerase III (Pol III) gene (*CD1305*). The relative change in gene expression was recorded as the ratio to normalized target concentrations (threshold cycle [$\Delta\Delta C_T$]) (41). The Shapiro-Wilk test was performed to test the normality of the replicates for each condition (see Table S3 in the supplemental material). When a population of the two conditions was normally distributed, a *t* test was used: otherwise, we used a Mann-Whitney test as indicated in the figure legends. A *P* value of ≤0.05 was considered significant.

Microarray design for the *C. difficile* genome, DNA array hybridization, and data analysis. The microarray of the *C. difficile* strain 630 genome was designed as previously described (15) (GEO database accession no. GPL10556). The transcriptomic analysis was performed with four different RNA preparations and a dye swap method. First, 10 μg of total RNA was reverse transcribed in cDNA using the SuperScript Indirect cDNA labeling system kit (Invitrogen) and Cy3 or Cy5 fluorescent dye (GE Healthcare) according to the manufacturer's recommendations. Labeled DNA hybridization to microarrays and array scanning were performed as previously described (15). All slides were analyzed using the R and limma software (Linear Model for Microarray Data) from the Bioconductor project (www.bioconductor.org). For each slide, we corrected for background with the "normexp" method (42), which resulted in strictly positive values and reduced variability in the log ratios for genes with low hybridization signal levels. Then, we normalized each slide by the "loess" method (43). To test for differential expression, we used Bayesian adjusted *t* statistics and performed the multiple testing correction of Benjamini and Hochberg based on the false discovery rate (FDR) (44). A gene was considered to be differentially expressed when the *P* value was <0.05.

Raw sequence analysis. The presence of the TCS locus (*CD2602* to *CD26021*) was inferred from raw sequences of 2,424 published strains (Sequence Read Archive [SRA] accession no. PRJEB2039, PRJEB4556, PRJEB3010, PRJEB190 to PRJEB216, PRJEB6600 to PRJEB6602, and PRJEB6575). For that purpose, we mapped the sequencing reads of each strain onto the nucleotide sequence of the TCS locus using Bowtie (1). A

strain was considered to contain the TCS locus when the coverage was above 80%.

Microarray data accession number. The complete experimental data set has been deposited in the GEO database under accession no. GSE22423.

RESULTS AND DISCUSSION

Cysteine-dependent repression of PaLoc genes. It has been shown that toxin synthesis is repressed by cysteine in the high-toxin-level-producing strain VPI 10463 (12). To determine whether the effect of cysteine on toxin synthesis is strain dependent, we measured the effect of cysteine on toxin production in several *C. difficile* backgrounds (Table 1), such as strains 630Δ*erm* and M7404 (a NAP1/027 epidemic strain), as well as an M7404 derivative strain carrying a wild-type copy of the *tcdC* gene on the pDLL17 plasmid (2); VPI 10463 was used as a control. All of the strains grew similarly in PY with or without cysteine. Cell crude extracts were obtained from these four strains after 10 h of growth in PY or PYC, and toxin production was assayed by Vero cell cytotoxicity assays, which predominantly assess TcdB, and protein dot blot analysis using a specific antibody raised against TcdA. Cytotoxic activity was lower in cells grown in the presence of cysteine (Fig. 2A) than in cells grown without cysteine, with 25- to 125-fold decreased cytotoxicity for strains 630Δ*erm*, M7404, and M7404(pDLL17-*tcdC*) and 16,000-fold decreased cytotoxicity for strain VPI 10463. Moreover, TcdA accumulation was strongly reduced in the presence of cysteine in all of the strains tested (Fig. 2B). These results suggest that cysteine-dependent repression of toxin production is conserved among the *C. difficile* strains. Cysteine repressed toxin synthesis in both the epidemic 027 strain M7404, which does not express functional TcdC, and in its derivative strain that contains a wild-type *tcdC* gene (2). Thus, the effect of cysteine on toxin production is not mediated by TcdC.

To determine whether the effect of cysteine on toxin production occurred at the transcriptional level, we performed qRT-PCR experiments for the *tcdA*, *tcdB*, and *tcdR* genes using strain 630Δ*erm* (Fig. 2C). After 10 h of growth, the transcript levels of *tcdA* and *tcdB* decreased 18- and 17-fold, respectively, in the presence of cysteine. We also observed that the expression of the *tcdR* gene encoding the alternative sigma factor required for toxin gene transcription decreased 40-fold when cysteine was added (Fig. 2C). These data are in agreement with the results obtained by Karlsson et al. (11), suggesting that toxin gene transcription is repressed by cysteine through negative regulation of *tcdR*.

Reconstruction of sulfur metabolism in *C. difficile*. An understanding of sulfur metabolism was a prerequisite to elucidating how cysteine negatively regulates toxin production. To reconstitute the sulfur metabolism pathways, we first searched for all of the gene homologs to the genes involved in sulfur assimilation pathways in other firmicutes (30) in the complete genome sequence of the reference *C. difficile* strain 630 (45) (Fig. 3). All genes identified are conserved in the VPI 10463 and NAP1/027 epidemic strains (see Table S4 in the supplemenal material). Then, to support the metabolic reconstruction and to obtain new insights into the physiology of *C. difficile*, we tested the ability of strain 630Δ*erm* to grow in minimal media with different sulfur sources (Table 2).

Strain 630Δ*erm* cannot grow when sulfate is the only sulfur source (Table 2). This finding is consistent with the absence of genes involved in the first steps of the sulfate assimilation pathway leading to sulfite (Fig. 1). In contrast, strain 630Δ*erm* was able to grow in the presence of sulfide or thiosulfate (Table 2), indicating that *C. difficile* can synthesize cysteine from these compounds, probably through the CysE/CysK thiolation pathway (Fig. 3). Cysteine can also be produced from glutathione, a sulfur source utilized by strain 630Δ*erm* (Table 2). PepT and PepA are probably involved in the degradation of glutathione to form cysteine (Fig. 3). However, the pathway of glutathione synthesis from cysteine that is found in *C. perfringens* (20) is absent in *C. difficile*. Strain 630Δ*erm* can also grow with cysteine as the sole sulfur source, indicating that methionine is efficiently produced from this compound. As shown in Fig. 3, methionine is synthesized from homocysteine, likely through the cobalamine-dependent methionine synthase MetH. The two main pathways of homocysteine produc-

A

	630Δ*erm*	M7404	M7404 (*tcdC*+)	VPI10463
PYC/PY	4.10^{-2}	4.10^{-2}- 8.10^{-3}	4.10^{-2}- 8.10^{-3}	$6.3.10^{-5}$

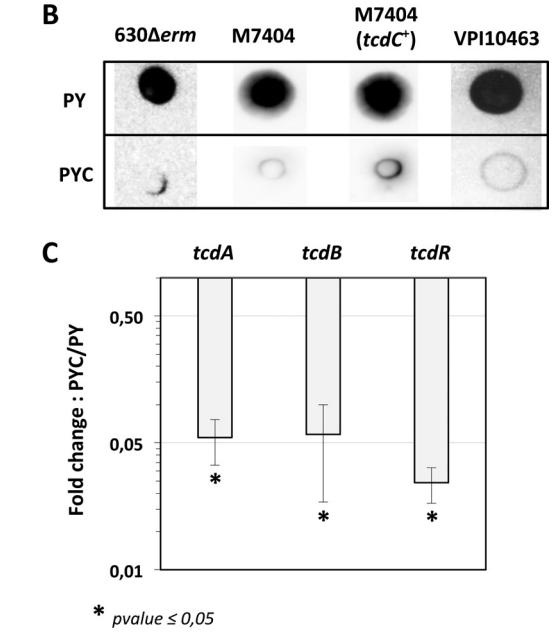

FIG 2 Effect of cysteine on toxin production in different *C. difficile* strains. (A) Cytotoxicity assays on Vero cells. Twofold serial dilutions of intracellular bacterial crude extracts were performed, and the dilutions were added to a 96-well plate of confluent Vero cells. The toxin titer corresponds to the lowest dilution of *C. difficile* crude extracts required for >50% cell rounding. Cytotoxicity results are presented as the ratio of the toxin titers of bacterial cells grown in the presence of cysteine (PYC) to those of bacterial cells grown in the absence of cysteine (PY). (B) TcdA dot blot analysis. The crude extracts of *C. difficile* strains (200 ng for strains 630Δ*erm*, M7404, and M7404 complemented with pDLL17-*tcdC* and 20 ng for strain VPI 10463) were probed with anti-TcdA antibodies as described in Materials and Methods. The results presented are representative of crude extracts tested from at least three independent experiments. (C) Transcript levels of the *tcdR*, *tcdA*, and *tcdB* genes in strain 630Δ*erm* grown in the presence or absence of cysteine. Results are presented as the ratio of the mRNA level (arbitrary units) of each gene in bacterial cells grown in the presence of cysteine (PYC) to that of each gene in cells grown in the absence (PY) of cysteine. The results are the averages from at least three independent experiments, and error bars are the standard deviations from the mean values. The statistical analysis was performed by using a *t* test (*tcdA* and *tcdR*) or a Mann-Whitney test (*tcdB*).

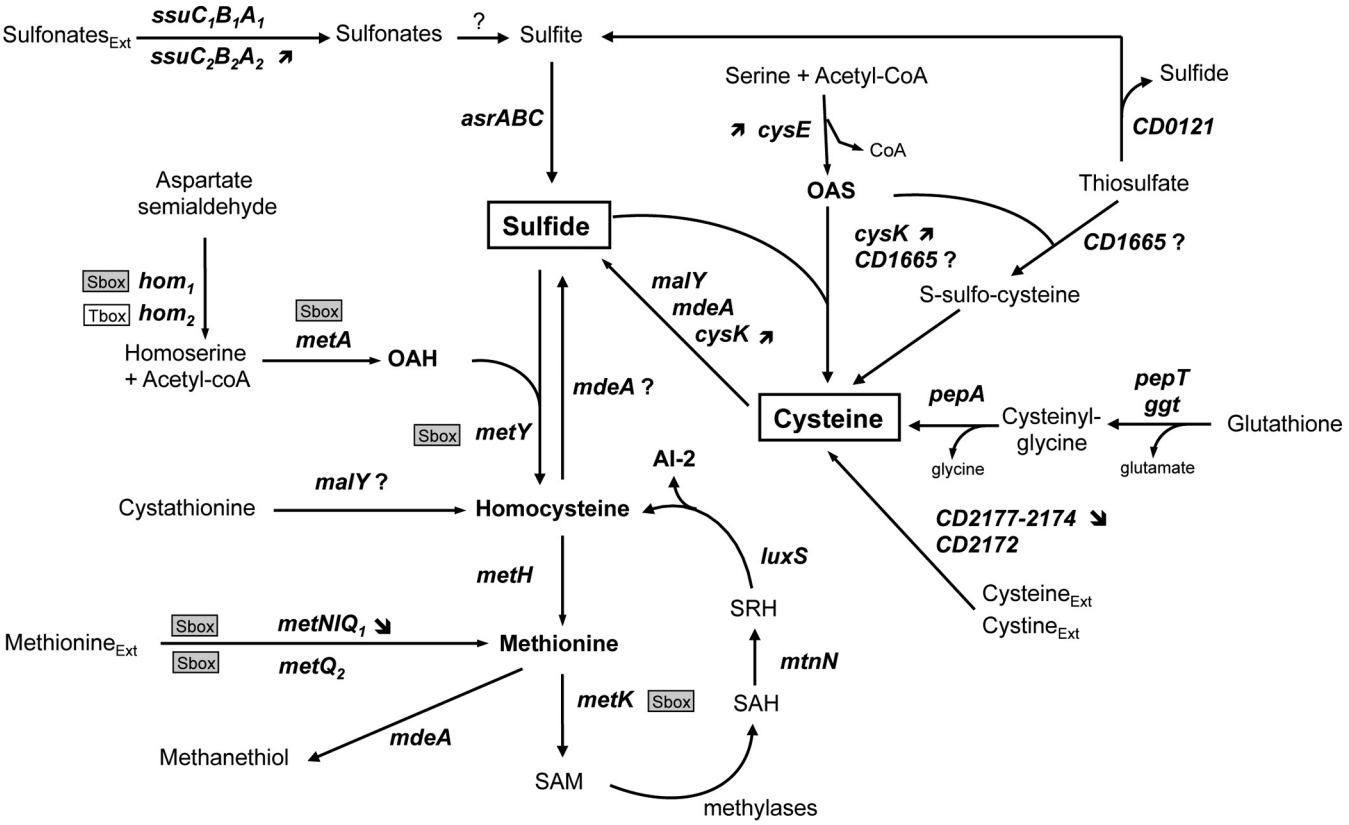

FIG 3 Reconstruction of sulfur metabolism in *C. difficile*. Genes of strain 630Δ*erm* are renamed on the basis of *B. subtilis* orthologs. The genes and their products are as follows: *cysE*, serine *O*-acetyltransferase (CD1595); *cysK*, OAS-thiol-lyase (CD1594); *asrABC*, anaerobic sulfite reductase (CD2231 to -2233); *ssuCBA*$_1$, ABC-transport system sulfonates (CD1482 to -1484); *ssuCBA*$_2$, ABC-transport system sulfonates (CD2989 to -2991); *metA*, homoserine acetyl-transferase (CD1826); *metY*, OAH thiol-lyase (CD1825); *malY*, cystathionine β-lyase (CD3029); *metH*, cobalamin-dependent methionine synthase (CD3596); *metK*, SAM synthetase (CD0130); *mtnN*, adenosylhomocysteine nucleosidase (CD2611); *luxS*, *S*-ribosylhomocysteine lyase (CD3598); *mdeA*, methionine γ-lyase (CD3577), *metNIQ*$_1$, ABC transport system methionine (CD1489 to -1491); *pepT*, peptidase T (CD1046); *pepA*, leucine aminopeptidase (CD1300). Other abbreviations: AI-2, autoinducer 2; OAS; *O*-acetylserine; OAH, *O*-acetylhomoserine; SAM, *S*-adenosyl-methionine; SAH, *S*-adenosyl-homocysteine; SRH, *S*-ribosyl-homocysteine; Ext, external. As indicated, an S-box motif is located upstream of the *metY-metA* and *metNIQ*$_1$ operons and of the *metQ*$_2$ and *metK* genes, suggesting that they are controlled by a SAM-dependent riboswitch (55). A T box is present upstream of *hom-CD1580*.

tion in bacteria are transsulfuration and thiolation (Fig. 1) (30). Both pathways involve PLP-dependent enzymes: transsulfuration requires a cystathionine γ-synthase and a cystathionine β-lyase, while thiolation requires an *O*-acetyl-homoserine (OAH)-thiol-lyase (Fig. 1). In the genome of strain 630, three PLP-dependent enzymes were identified by their similarities: MetY, MalY, and MdeA (46). MetY contains an amino acid insertion specific to OAH-thiol-lyases, MalY is a cystathionine β-lyase of the PatB/MalY family (32), and MdeA is a probable methionine γ-lyase. However, no cystathionine γ-synthase is present in *C. difficile*, suggesting that a functional transsulfuration pathway is absent and that *C. difficile* synthesizes both methionine and cysteine by thiolation pathways.

Homocysteine and cysteine degradation. Strain 630Δ*erm* can grow in the presence of homocysteine and, to a lesser extent, in the presence of cystathionine but cannot use methionine as the sole sulfur source (Table 2). The ability to use homocysteine is surprising because the reverse transsulfuration pathway, which involves a cystathionine β-synthase and a cystathionine γ-lyase (Fig. 1), is absent in *C. difficile* (31, 47). Growth in the presence of homocysteine could be explained by the existence of a homocysteine γ-lyase, allowing the production of H_2S from homocysteine and its possible conversion into cysteine (Fig. 3). Using lead-acetate paper, we detected the production of H_2S during the growth of strain 630Δ*erm* in PY plus homocysteine (PYHC), but not in PY alone (Fig. 4A). When we performed zymography using homocysteine as a substrate, we detected a single band in crude extracts of strain 630Δ*erm* grown in PY, PYC, and PYHC (Fig. 4B), suggesting that homocysteine γ-lyase activity is induced under all of the growth conditions used. Among the PLP-dependent enzymes encoded by the *C. difficile* genome, MdeA shares significant similarities with the methionine γ-lyases of *Citrobacter freundii* (48) and of *Brevibacterium linens*. Interestingly, the methionine γ-lyase of *B. linens* also has homocysteine γ-lyase activity (49), making MdeA a probable candidate for the production of H_2S from homocysteine and the degradation of methionine to form methanethiol in *C. difficile* (Fig. 3), as previously proposed (50).

In bacteria, cysteine is usually catabolized by cysteine desulfhydrases (32), producing H_2S, pyruvate, and ammonia (Fig. 1). We detected high production of H_2S during the growth of strain 630Δ*erm* in PYC (Fig. 4A). Indeed, the quantification of H_2S showed a 20- to 30-fold increase of H_2S production when cysteine was added to the medium (Fig. 4C). This result clearly indicated that cysteine is efficiently degraded in *C. difficile*. To detect the

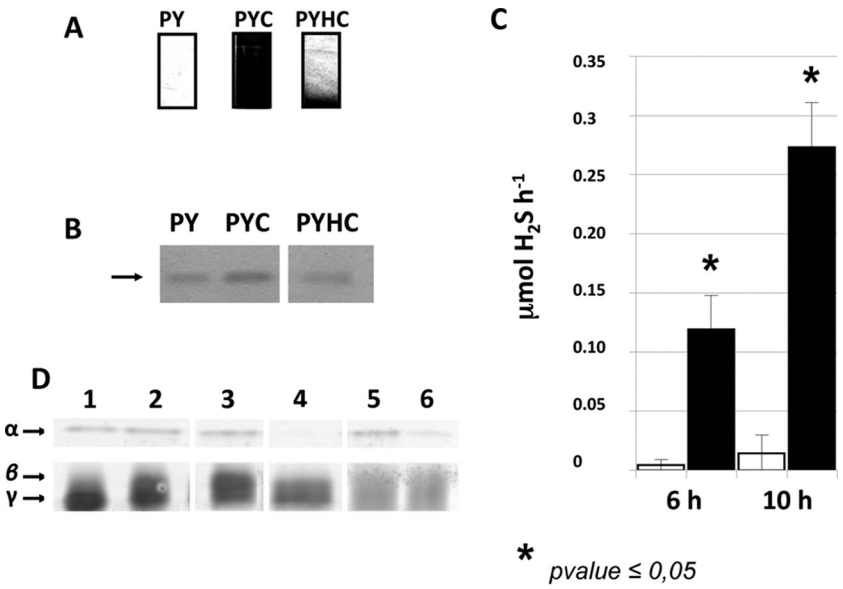

FIG 4 Hydrogen sulfide production in strain 630Δ*erm*. (A) Detection of H_2S production using lead-acetate paper. H_2S production was evaluated in the media PY, PY plus cysteine (PYC), and PY plus homocysteine (PYHC). The production of H_2S yielded a black color due to the formation of PbS. (B) Detection of the homocysteine γ-lyase activity on a zymogram. Crude extracts of strain 630Δ*erm* grown in PY, PYC, or PYHC were loaded on a native polyacrylamide gel (12%) and incubated with 10 mM homocysteine. Homocysteine γ-lyase was detected by the formation of insoluble PbS via the release of H_2S. Lanes of the zymogram have been reorganized from the same image to present data chronologically. (C) Quantitative detection of H_2S after 6 or 10 h of growth of strain 630Δ*erm* in PY (white boxes) or PYC (black boxes). H_2S production was measured using the quantitative methylene blue method, as described in Materials and Methods. The statistical analysis was performed by using the Mann-Whitney test for all genes. (D) Detection of cysteine desulfhydrase activities on a zymogram. Crude extracts of strain 630Δ*erm* (lanes 1 and 2), 630Δ*erm*::*cysK* (lane 3), 630Δ*erm*::*sigL* (lane 4), 630Δ*erm*(pRPF185) (lane 5), and 630Δ*erm*(pDIA6456-AS*malY*) (lane 6). The strains were grown in PY (lane 1) or PYC (lanes 2 to 6). Samples were charged on a native polyacrylamide gel (12%) and incubated with 10 mM cysteine. The cysteine desulfhydrases were detected by the formation of insoluble PbS formed by the release of H_2S. The results presented are representative of at least three independent experiments. Lanes of the zymogram have been reorganized from the same image to present data chronologically.

cysteine desulfhydrase activities, we performed zymography using L-cysteine as the substrate. We detected two bands (α and γ) in the crude extract of strain 630Δ*erm* grown in PY (Fig. 4D, lane 1). Interestingly, when strain 630Δ*erm* was grown in PYC, we detected an additional band (β), indicating that synthesis of this desulfhydrase enzyme was induced by cysteine (Fig. 4D, lane 2). In *B. subtilis*, PatB/MalY- and CysK-type enzymes have cysteine desulfhydrase activities (32). To determine whether CysK of *C. difficile* is a cysteine desulfhydrase, we inactivated the *cysK* gene in strain 630Δ*erm* using the ClosTron system (see Fig. S1 in the supplemental material). The zymogram profile obtained with the *cysK* mutant strain grown in PYC is similar to that obtained with the 630Δ*erm* strain (Fig. 4D, lane 3). This finding suggests that CysK is not a major cysteine desulfhydrase in *C. difficile* under the conditions tested, although we cannot exclude a role for CysK in cysteine degradation. We failed to inactivate the gene encoding the PatB/MalY enzyme, probably because of its essentiality for *C. difficile* (51). Thus, to evaluate whether PatB/MalY is a cysteine desulfhydrase, we constructed a PatB/MalY-depleted strain using an antisense strategy (36, 52). Compared to the strain carrying the control plasmid (Fig. 4D, lane 5), the PatB/MalY-depleted strain (Fig. 4D, lane 6) displayed a decreased intensity of the α band, suggesting that MalY has cysteine desulfhydrase activity. However, the enzymes with cysteine desulfhydrase activity corresponding to the γ and β bands on the zymogram (Fig. 4D) remain to be identified.

Finally, we demonstrated that both homocysteine and cysteine are actively catabolized by *C. difficile*. Interestingly, it has recently been shown that when *C. difficile* grows in minimal medium with Casmino Acids, cysteine is consumed immediately and sulfide is produced (53). This finding is in complete agreement with our results. Thus, we propose that sulfide is a central compound of sulfur metabolism in *C. difficile*, as it is the direct precursor of both methionine and cysteine, as well as the major degradation product of the sulfur-containing amino acids homocysteine and cysteine (Fig. 3).

Global analysis of gene expression in response to cysteine. To determine the global impact of cysteine on gene expression and to elucidate the mechanism of cysteine-dependent repression of toxin production, we performed a comparative transcriptional analysis of strain 630Δ*erm* grown in PY or PYC at the onset of the stationary phase (10 h). In the presence of 10 mM cysteine, 6% of the genome (201 genes) was differentially expressed with a fold change of ≥2 (see Table S2 in the supplemental material). Among these genes, 120 and 81 were upregulated and downregulated, respectively. The major expression changes were seen in genes encoding cell-surface-associated proteins and proteins involved in sulfur, amino acid, carbon, and energy metabolism as well as in iron uptake (see Table S2). The transcriptomic analysis confirmed that toxin gene expression decreased in the presence of cysteine. In addition, exposure of *C. difficile* to high cysteine concentrations strongly induced the expression of genes encoding heat shock proteins belonging to both class I (HrcA dependent), such as the *groESL* and *hrcA* operons, and class III (CtsR dependent), such as the *ctsR* and the *clpB* operons. We validated the transcriptomic analysis by performing qRT-PCR with a selection of 12

representative genes. The results confirmed the microarray data (see Table S2).

Regulation of genes involved in sulfur metabolism and in thiol protection by cysteine. As expected, the expression of genes related to sulfur metabolism, including transporters of amino acids, was controlled by cysteine. The *metQ*$_1$ gene encoding the methionine-binding protein of an ABC transporter (54, 55) (Fig. 3) was less strongly expressed in PYC. This gene is probably regulated by an S-box riboswitch in the promoter region of the *metN*$_1$*Q*$_1$ operon, like most of the genes required for methionine uptake (Fig. 3) (55, 56). The ABC transporter system composed of CD2177, CD2176, CD2175, CD2174, and CD2172 is likely involved in the uptake of cystine and/or cysteine in *C. difficile* (Fig. 3). CD2177 and CD2174 share similarities with the cystine-binding proteins of *E. coli* and *Bacillus subtilis* (57), while CD2176 and CD2175 are similar to the L-cystine permeases of *E. coli* and *B. subtilis*. The expression of all of the genes encoding this ABC transporter decreased 2.5- to 4-fold in PYC, as is usually observed for cysteine/cystine transporters. In contrast, the expression of the *ssuA*$_2$ and *ssuC*$_2$ genes, which encode proteins sharing similarities with sulfonate ABC transporters, increased in the presence of cysteine (Fig. 3).

The expression of *cysK*, encoding the OAS-thiol-lyase, and *cysE*, encoding the serine acetyl-transferase was induced 40- to 50-fold in the presence of cysteine (Fig. 3; see Table S2 in the supplemental material). The upregulation of *cysKE* expression in PYC is surprising because CysK and CysE, which are required for cysteine biosynthesis, are usually induced during cysteine limitation, as previously observed in *C. perfringens*, *B. subtilis*, *E. coli*, and *Salmonella* (20, 30, 34). However, in the presence of high cysteine concentrations, CysK contributes to cysteine degradation rather than cysteine synthesis (58). Under these conditions, CysE activity is inhibited by feedback, as established in several bacteria and plants (38, 59). Nonetheless, the role of CysK in cysteine metabolism remains to be clarified.

Finally, we observed that genes involved in thiol protection were induced in the presence of cysteine (see Table S2 in the supplemental material). They encode two thioredoxins (*CD1690* and *CD2355*), a thioredoxin reductase (*CD1691*), and a thiol peroxidase (*CD1822*). The induction of genes involved in thiol protection and in the stress response suggests that cysteine or its derivative products (e.g., H_2S) stress *C. difficile*. However, the addition of 10 mM cysteine to the PY medium did not affect *C. difficile* growth and cell viability (data not shown), while this amino acid is toxic in other bacteria, such as *E. coli* and *B. subtilis* (60; I. Martin-Verstraete, unpublished results). The expression of the stress-responsive genes in relation to the absence of cysteine toxicity in *C. difficile* may be the result of an adaptation to an anaerobic lifestyle.

Induction of *fur* and Fur-regulated genes in the presence of cysteine. The ferric uptake regulator (Fur) protein is an iron response repressor that controls the expression of genes involved in iron transport in bacteria (61, 62). The CD1287 protein shares 48% identity with the Fur protein of *B. subtilis*. To demonstrate that CD1287 corresponds to Fur, we constructed a *CD1287* mutant strain using the ClosTron system (see Fig. S1 in the supplemental material). Then, we tested the effect of *CD1287* disruption on the level of transcription of the *feoB1* and *fhuD* genes by qRT-PCR. In *B. subtilis*, FeoB1 and FhuD participate in ferrous iron and ferrichrome uptake, respectively (61, 63). We showed that the addition of 200 μM dipyridyl, a ferrous iron chelator, to the growth medium increased the transcript level of the *CD1287*, *fhuD*, and *feoB1* genes and that transcription of *feoB1* and *fhuD* increased 3,500- and 45-fold, respectively, in the *CD1287* mutant compared to the wild-type strain (data not shown). These results strongly indicate that CD1287 is the Fur repressor in *C. difficile*, as recently demonstrated (64).

From our global transcriptomic analysis, we found that the presence of cysteine in the medium induced the Fur regulon, including *fur* and genes encoding transporters of ferrous iron and ferrichrome (Table 3). Using the Fur-binding site of *B. subtilis* (61), we detected a potential Fur box upstream of approximately 20 genes that are differentially expressed in PYC, including *fur*, *feoB1*, *cysK*, and *fhuD*, as well as genes encoding proteins of unknown function, such as *CD2992*, *CD1485*, *CD2499*, and *CD2881* (Table 3). The consensus Fur box for *C. difficile* (Fig. 5A), deduced from the putative Fur-binding motifs present in the regulatory region of these genes, is highly similar to that defined by Ho et al. (64). We then tested the effect of cysteine on the transcription of some of these Fur targets by qRT-PCR in both 630Δ*erm* and a *fur* mutant strain. In the presence of cysteine, the transcript levels of the *fur*, *feoB1*, *cysK*, *fhuD*, and *CD2992* genes increased 3.2-, 750-, 56-, 12-, and 10-fold, respectively, in strain 630Δ*erm* (Fig. 5B), a result consistent with the transcriptome data (Table 3). The cysteine-dependent upregulation of *feoB1*, *fhuD*, and *CD2992* was abolished in the *fur* mutant, indicating that the effect of cysteine is mediated by the Fur repressor. Interestingly, the induction of *cysK* transcription by cysteine was not completely abolished in the *fur* mutant and was only 5-fold lower than it was in strain 630Δ*erm* (Fig. 5B). In addition, in the absence of cysteine, the transcript level of *cysK* was 4.5-fold higher in the *fur* mutant than in strain 630Δ*erm* (data not shown). As a Fur box is located in the promoter region of the *cysK* gene, the regulation of *cysK* by cysteine is complex, involving both direct regulation by the Fur repressor and control by a still-uncharacterized regulator. While very few data concerning the control of *cysK* expression by Fur are available (65), the cysteine-dependent regulation of CysK synthesis in *C. difficile* seems to be atypical.

The induction of the Fur regulon by cysteine suggests that the presence of cysteine in the growth medium mimics the conditions of iron depletion. A black precipitate appears when strain 630Δ*erm* is grown in PYC (Fig. 5C). This finding is consistent with the production of high levels of H_2S via cysteine degradation by cysteine desulfhydrases (Fig. 4C), which probably leads to the formation of this black deposit from iron-sulfide precipitation. This phenomenon is often described in anaerobic waste collection systems (66). Therefore, iron depletion due to the precipitation of iron in the presence of excess sulfide can explain the induction of the Fur-regulated genes.

Regulation by cysteine of carbon and energy metabolism. The ability of *C. difficile* to use a wide range of carbohydrates might be important during infection. Accordingly, Antunes et al. (13) demonstrated the existence of links between carbon metabolism and toxin production. The addition of cysteine to the medium increased the expression of several genes of carbon metabolism, including genes encoding phosphotransferase systems (PTS) and genes encoding enzymes involved in the second part of glycolysis (Fig. 6A; see Table S2 in the supplemental material).

The expression of genes involved in the fermentation pathways of *C. difficile* was also modulated by the presence of cysteine (Fig. 6A). Thus, the expression of *ldh* and *buk*, which encode lactate

TABLE 3 List of the Fur regulon genes differentially expressed in PY and PYC with a putative Fur box in their promoter region

Gene	Protein function	PYC/PY ratio	Fur box position[a]
CD1287 (*fur*)	Ferric uptake regulation protein	3.3	−38
CD1477 (*feoA*)	Ferrous iron transport protein A	64.1	
CD1478 (*feoA1*)	Ferrous iron transport protein A1	107.0	
CD1479 (*feoB1*)	Ferrous iron transport protein B1	127.1	−60
CD1480	Putative exported protein	162.6	
CD1745A (*feoA*)	Ferrous iron transport protein A	16.7	−30
CD3273 (*feoA3*)	Ferrous iron transport protein A	13.4	−30
CD3274 (*feoB3*)	Ferrous iron transport protein B	12.1	
CD2878 (*fhuD*)	ABC transporter, ferrichrome substrate-binding protein	NA[b]	−47
CD2875 (*fhuC*)	Ferrichrome ABC transporter	3.0	
CD1594 (*cysK*)	*O*-Acetyl-serine sulfhydrylase	43.0	−162
CD1595 (*cysE*)	Serine acetyltransferase	44.0	
CD1999 (*fldX*)	Flavodoxin	28.5	−158
CD1777	Putative arsenate reductase	3.3	−80
CD1485	Conserved hypothetical protein	6.9	−34
CD2499	Conserved hypothetical protein	15.4	−34
CD2881	Conserved hypothetical protein	2.6	−58
CD2992	Conserved hypothetical protein	2.5	−36
CD2991	ABC transporter, sulfonate-permease	3.5	
CD2989	ABC transporter, sulfonate-extracellular solute-binding protein	4.8	

[a] The position of the Fur box is indicated according to the translational start site of the corresponding gene.
[b] NA, not detected in transcriptome.

dehydrogenase and one butyrate kinase, respectively, decreased, while the expression of genes encoding pyruvate formate lyases and an alcohol dehydrogenase increased in the presence of cysteine. Surprisingly, the *bcd2* operon, which is involved in the production of butyryl coenzyme A (butyryl-CoA) from acetyl-CoA (Fig. 6A), was not differentially expressed in the transcriptome analysis. However, when we tested the effect of cysteine on the expression of the *bcd2* and *hbd2* genes by qRT-PCR, we showed that their transcript levels decreased 5.5- and 6-fold in PYC compared to PY, respectively. This result is in agreement with the results of a proteome analysis performed in strain VPI 10463 (12), showing that the production of enzymes involved in the conversion of acetyl-CoA to butyryl-CoA (Bcd2, Crt2, and Hbd) decreases when cells are grown in the presence of cysteine. To evaluate the impact of cysteine on fermentation pathways, we quantified the end products of fermentation in strain 630Δ*erm* grown over 48 h in PY or PYC by gas-liquid chromatography. The amounts of lactate and butyrate were reduced 4- and 6-fold, respectively, in the presence of cysteine (see Fig. S2 in the supplemental material), as observed in strain VPI 10463 (12). This result is consistent with the downregulation of *ldh*, *buk*, and *bcd2* operon expression. After 48 h of growth, butyric acid production was high in PY, leading to a final concentration of 5 mM compared to less than 1 mM in PYC (see Fig. S2). Interestingly, the addition of butyric acid to the growth medium enhances toxin production in strain VPI 10463 (12). Thus, the addition of cysteine to the medium may indirectly control toxin production at least partly via its influence on butyric acid production. However, the molecular mechanisms of the regulation of toxin synthesis in response to butyric acid availability remain to be determined.

Control of amino acid metabolism by cysteine. To analyze the impact of cysteine on amino acid metabolism, we compared the transcriptome and the pools of amino acids obtained from strain 630Δ*erm* grown in PY or PYC. A total of 32 genes involved in peptide or amino acid metabolism were differentially expressed under these two conditions (see Table S2 in the supplemental material), while the intracellular concentrations of leucine, tyrosine, alanine, valine, phenylalanine, and glutamic acid were increased in the presence of cysteine (Table 4). The expression of several genes involved in peptide degradation (*CD0779*, *CD2613*, *CD2347*, *CD2173*, and *CD0166*) and amino acid uptake (*CD2612*, *CD3092*, and *CD0165*) was differentially regulated when cysteine was added to the medium (Fig. 6A). In *C. difficile*, amino acid catabolism by the Stickland reactions can be a primary source of energy when bacteria are grown with amino acids as the sole carbon and nitrogen sources (67). Stickland reactions couple the metabolism of a pair of amino acids, of which one serves as the Stickland donor (alanine, valine, leucine, or isoleucine) and is oxidatively deaminated or decarboxylated to generate ATP and reducing power (NADH), and the second serves as the Stickland acceptor (glycine, proline, hydroxyproline, or leucine) and is reduced or reductively deaminated, regenerating NAD^+ from NADH (Fig. 6B). The genes encoding the glycine reductase (*grd*) and D-proline reductase (*prd*) operons, which are involved in the reduction of the Stickland acceptors glycine and proline, were induced up to 10-fold in the presence of cysteine (Fig. 6B; see Table S2). Interestingly, the expression of *proC* (*CD3281*), which is involved in the conversion of ornithine into proline, and of *CD2347*, which encodes a peptidase sharing similarities with Xaa-Pro dipeptidases and potentially generates free proline for use in the Stickland reactions (67), was also increased in the presence of cysteine.

In strain 630Δ*erm* grown in the presence of cysteine, we observed a substantial accumulation of alanine (Table 4), a by-product of cysteine catabolism. Indeed, cysteine is first converted into pyruvate through cysteine desulfhydrases; pyruvate is then converted into alanine by alanine aminotransferases (Fig. 6A). CD2828, which shares similarities with an alanine aminotransfer-

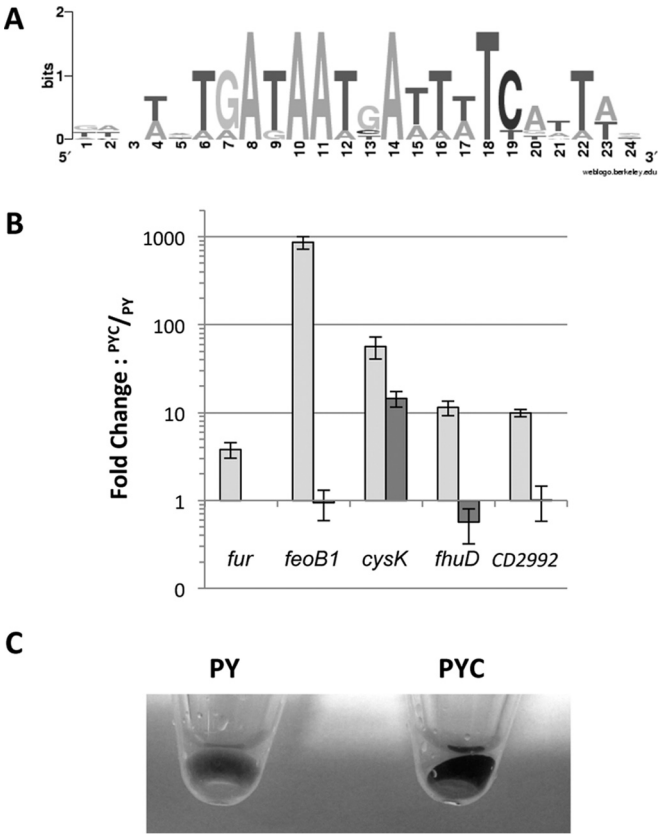

FIG 5 Analysis of Fur-regulated genes induced in the presence of cysteine. (A) Consensus sequence of the Fur box motif of *C. difficile*. The sequence logo was created by the alignment of putative Fur-regulated genes induced in the presence of cysteine on the WebLogo website (http://weblogo.berkeley.edu). The height of the nucleotides is proportional to their frequency. (B) Effect of cysteine on the transcript level of *fur* (*CD1287*), *feoB1* (*CD1479*), *cysK* (*CD1594*), *fhuD* (*CD2878*), and *CD2992* in 630Δ*erm* and the 630Δ*erm*::*fur*. The 630Δ*erm* (white boxes) and 630Δ*erm*::*fur* (black boxes) strains were grown for 10 h in PY or PYC. qRT-PCR results are presented as the ratio of the amount of mRNA (arbitrary units) of each gene in bacterial cells grown in PYC to that of each mRNA in the bacterial cells grown in PY. Data are the averages from at least three independent experiments, and error bars are the standard deviations from the mean values. (C) Aspect of the bacterial pellet of strain 630Δ*erm* grown for 10 h in PY or in PYC. The black precipitate is due to FeS precipitation.

ase characterized in *E. coli* (68), is a good candidate for this activity. However, *CD2828* was repressed in PYC (see Table S2 in the supplemental material). The negative control of *CD2828* expression in the presence of a high intracellular concentration of alanine might explain this downregulation.

Several genes involved in the biosynthesis of branched-chain amino acids (BCAAs) were also repressed by cysteine (Fig. 6A; see Table S2 in the supplemental material). The expression of *ilvD* involved in the BCAA synthesis from pyruvate and of the *leuABCD* operon, which is involved in synthesis of leucine, was downregulated 5- to 10-fold in the presence of cysteine. Interestingly, the transcription of *brnQ1*, which encodes a BCAA transporter (Fig. 6A), was also decreased in PYC. A T box specific to leucine (T box_{Leu}) is present in the promoter region of the *leuABCD* operon and of the *leuS* gene, indicating that these genes are probably induced during leucine starvation via premature termination of transcription (56, 69). We note that *ilvD*, *leuABCD*, and *brnQ1* belong to the CodY regulon, which is involved in the adaptive response to nutrient limitation (17). Thus, the increase in the concentration of valine and leucine when cysteine is added (Table 4) might lead to the repression of genes involved in BCAA biosynthesis and uptake through their control by a T box_{Leu} or by CodY. In *B. subtilis*, changes in the rate of endogenous isoleucine, leucine, and valine synthesis modulate the expression of CodY-regulated genes (70). In addition, for *Clostridum sticklandii*, using amino acids as the carbon and energy sources, cysteine is one of the six amino acids that is preferentially degraded, while valine, leucine, and isoleucine are used later, suggesting that certain amino acids regulate the metabolism of others (71). Cysteine is also one of the three amino acids that are preferentially used by *C. difficile* (53). Our results suggest that the presence of cysteine may delay the use of other amino acids, such as BCAAs, which are known to act as corepressors of CodY (17). Accordingly, we observed that 31 CodY-regulated genes were repressed in strain 630Δ*erm* when cysteine was added (see Table S2), suggesting that cysteine has an impact on CodY activity.

Involvement of regulators in the cysteine-dependent repression of toxin production. Toxin expression may be under the control of a global regulator that is able to sense cysteine availability. Interestingly, we showed that several genes encoding regulators are regulated in response to cysteine availability. Indeed, *CD0278*, *CD1692*, *CD2023*, and *CD2065* were up- or downregulated in the presence of cysteine (see Table S2 in the supplemental material). Using the ClosTron system, we inactivated *CD0278*, *CD2023*, and *CD2065*, but we did not succeed in disrupting *CD1692*. Compared to the wild-type strain, toxin gene expression was similarly repressed by cysteine in the *CD0278*, *CD2023*, and *CD2065* mutants (data not shown). However, we cannot exclude the possibility that a still-unidentified regulator intervenes in this control. Alternatively, the effector of cysteine-dependent regulation might be a cysteine by-product that is accumulated during growth in PYC. To discriminate between a direct effect of cysteine and an indirect metabolic effect, we added 10 mM cysteine to the growth medium for 1 h at the onset of the stationary phase. Surprisingly, under this condition limiting the catabolism of cysteine, we observed that the transcription of *tcdA*, *tcdB*, and *tcdR* was increased (see Fig. S3 in the supplememtal material), suggesting that cysteine downregulates toxin production through a product of cysteine degradation (see below). As changes in carbon source and amino acid availability were observed after the growth of *C. difficile* in the presence of cysteine (Table 4; see Fig. S2 in the supplemental material), we wondered whether toxin synthesis could be controlled by the global regulators CodY and CcpA, which are known to regulate toxin gene expression in response to the levels of the BCAAs and PTS sugars, respectively (13, 14, 18). However, we showed that toxin synthesis is similarly repressed by cysteine in the *codY* or *ccpA* mutant and wild-type strains (Fig. 7A), indicating that CodY and CcpA do not mediate the control of toxin synthesis by cysteine.

The Fur regulator might also be responsible for the cysteine-dependent regulation of toxin synthesis. Indeed, the expression of many virulence factors in pathogenic bacteria is negatively regulated by Fur in response to iron availability (72). We showed that TcdA production is repressed by cysteine in a *fur* mutant in the same manner as the wild-type strain (Fig. 7B), indicating that Fur is not involved in the downregulation of toxin production in PYC.

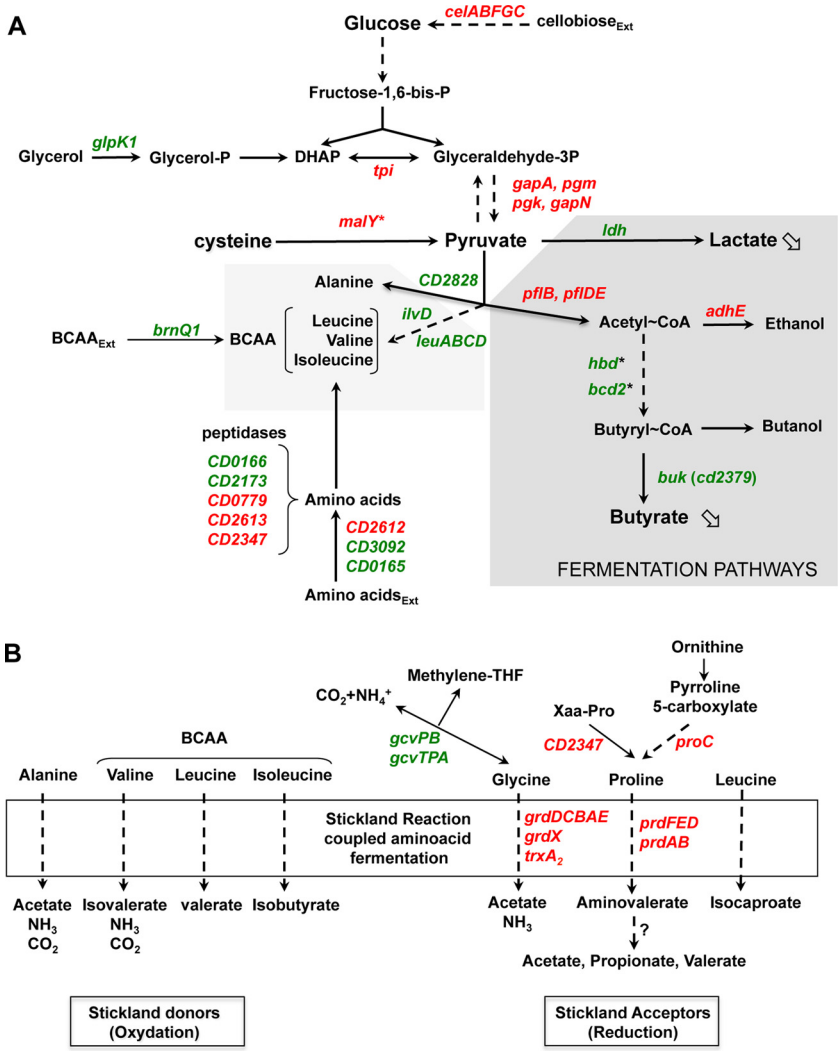

FIG 6 Overview of *C. difficile* genes involved in carbon and amino acid metabolism that are differentially expressed in the presence of cysteine. Genes that are up- and downregulated in the presence of cysteine in the transcriptome analysis are indicated in red and green, respectively. An asterisk indicates that the differential transcript level was detected by qRT-PCR. (A) Carbon metabolism and fermentation pathways. Assignments of genes (listed with their products) regulated by cysteine availability are as follows: *tpi*, triosephosphate isomerase; *gapA*/*gapN*, glyceraldehyde-3-phosphate dehydrogenase; *pgk*, phosphoglycerate kinase; *pgm*, 2,3-bisphosphoglycerate-mutase; *celABC*, PTS cellobiose; *celF*, cellobiose-6-P hydrolase; *ldh*, lactate dehydrogenase; *adhE*, aldehyde-alcohol dehydrogenase; *pflB* and *pflD*, pyruvate formate lyase; *pflE* and *pflA*, pyruvate formate lyase activating enzyme; *thiA1*, acetyl-CoA acetyltransferase; *bcd2*, butyryl-CoA dehydrogenase; *hbD2*, 3-hydroxybutyryl-CoA dehydrogenase; *crt2*, 3-hydroxybutyryl-CoA dehydratase; *buk*, butyrate kinase; *malY*, cysteine desulfhydrase; *ilvD*, dihydroxy-acid dehydratase; *leuA*, 2-isopropylmalate synthase; *leuB*, 3-isopropylmalate dehydrogenase; *leuC*, 3-isopropylmalate dehydratase large subunit; *leuD*, 3-isopropylmalate dehydratase small subunit; *brnQ1*, BCAA transporter. (B) Stickland reactions and associated metabolism. Assignments of genes regulated in response to cysteine availability are as follows: *grdDCBAEX*, glycine reductase complex; *prdEDBA*, proline reductase; *prdF*, proline racemase; *CD2347*, putative Xaa-Pro dipeptidase; *proC*, pyrroline-5-carboxylate reductase, *gcvPB*, glycine decarboxylase; *gcvTPA*, bifunctional glycine dehydrogenase/aminomethyl transferase protein.

This result was in agreement with the absence of the toxin genes in the Fur transcriptome, as recently defined by Ho et al. (64).

Role of SigL in the cysteine-dependent repression of toxin production. In *C. difficile* strain VPI 10463, it has been proposed that several proteins induced under toxin-producing conditions (PY) might be controlled by SigL (11). The *sigL* gene encodes a sigma factor belonging to the SigL/RpoN/σ^{54} family, which is known to play an important role in metabolism, adaptation, and virulence (73–77). To evaluate the role of SigL in the cysteine-dependent regulation of toxin synthesis, we inactivated the *sigL* gene (see Fig. S1 in the supplemental material). When we compared the levels of toxin produced between the *sigL* mutant and the wild-type strain 630Δ*erm* by dot blot analysis, we first observed that TcdA was produced at higher levels in the *sigL* mutant than in the wild-type strain when the cells were grown in PY medium (Fig. 7B). This effect might be due to decreased competition between SigL and the toxin-specific sigma factor TcdR for the core enzyme of the RNA polymerase, as already proposed for SigH (15). Surprisingly, we observed similar levels of TcdA production in the *sigL* mutant grown in PY and PYC (Fig. 7B). To determine whether SigL regulates toxin synthesis at the transcriptional level,

TABLE 4 Effect of cysteine addition on the intracellular concentration of amino acids in strain 630Δ*erm*

Amino acid	Amino acid concn (μmol/liter)		PYC/PY ratio[b]
	PY	PYC	
Upregulated in presence of cysteine			
Leucine	ND[a]	16.25 ± 1.6	+
Tyrosine	ND	20 ± 1.2	+
Alanine	13.5 ± 0.7	748 ± 40	55
Valine	5.3 ± 0.5	56.8 ± 1.3	10
Phenylalanine	2.6 ± 0.5	25.75 ± 5	10
Glutamic acid	19.3 ± 2	121.9 ± 9.5	6.5
Aminobutyric acid	8.5 ± 0.5	46.35 ± 0.8	5.5
Threonine	1.1 ± 0.1	2.4 ± 0.4	2.2
Serine	4 ± 0	9.85 ± 0.15	2.5
Asparagine	29.7 ± 2.6	59.7 ± 1.6	2
Methionine	4.85 ± 0.35	11.65 ± 1.65	2.5
Downregulated in presence of cysteine			
Cystathionine	1.2 ± 0.2	ND	−
Glutamine	11.8 ± 0.4	6 ± 0.1	0.5
Hydroxyproline	23.3 ± 1.5	13.9 ± 0.5	0.6

[a] ND, not detectable.
[b] +, detected only in PYC medium; −, detected only in PY medium.

we tested the transcription of the *tcdA*, *tcdB*, and *tcdR* genes in 630Δ*erm* and *sigL* mutant strains grown in PYC by qRT-PCR. As shown in Fig. 7C, the transcript levels of the *tcdA*, *tcdB*, and *tcdR* genes were approximately 25- to 50-fold higher in the *sigL* mutant than in the wild-type strain in the presence of cysteine. Moreover, complementation of the *sigL* mutant by a wild-type copy of *sigL* partially restored the cysteine-dependent repression of TcdA production (Fig. 7B) and of PaLoc gene transcription (Fig. 7C). These results indicate that SigL mediates the cysteine-dependent regulation of toxin gene expression. However, using the well-conserved consensus sequence of SigL-dependent promoters (78), we did not find a SigL-type promoter upstream of *tcdA*, *tcdB*, and *tcdR*, suggesting that SigL indirectly regulates the PaLoc genes, probably in response to an increase in the by-products of cysteine degradation. Indeed, using lead-acetate paper, we showed that the production of H_2S via cysteine degradation was strongly reduced in the *sigL* mutant compared to that in strain 630Δ*erm* (Fig. 8A) and was restored by complementation with pDIA6309. Interestingly, according to the zymogram profile obtained with the *sigL* mutant, we showed that the cysteine desulfhydrase activity of MalY (α band) significantly decreased (Fig. 4D, lane 4). In addition, the expression of *malY* was 4-fold lower in a *sigL* mutant than that in the wild-type strain (data not shown). This finding is in agreement with the role of SigL in the control of cysteine degradation in *C. difficile*. As pyruvate is the first product of cysteine degradation, we measured the extracellular concentration of pyruvate. We observed that in strain 630Δ*erm*, the pyruvate concentration increased more than 2-fold when we added cysteine to the medium. However, the level of pyruvate decreased 8-fold in the *sigL* mutant compared to the level in the wild-type strain (Fig. 8B). In addition, the *sigL* mutant strain complemented with the wild-type copy of *sigL* had an extracellular pyruvate concentration similar to that in strain 630Δ*erm* (Fig. 8B).

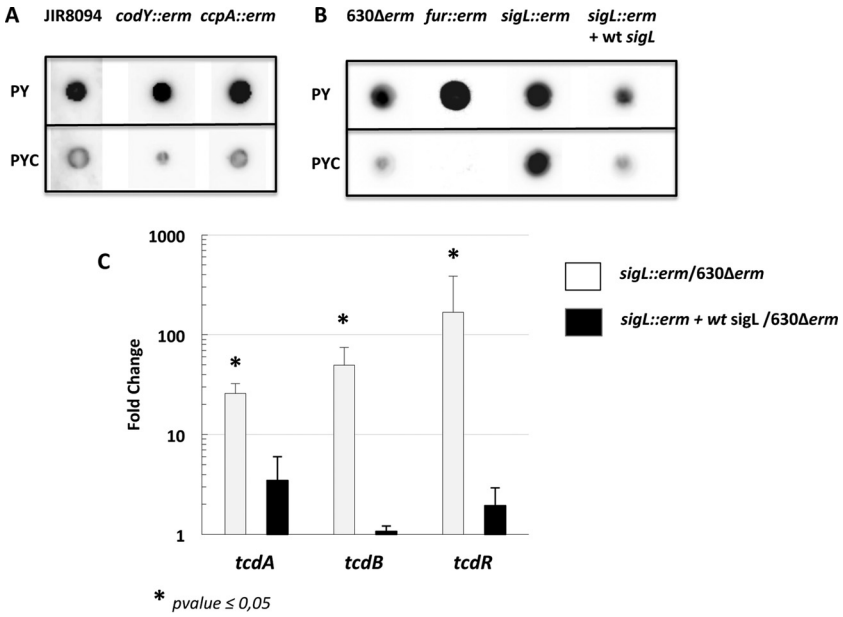

FIG 7 Role of Fur, CcpA, CodY, and SigL in the cysteine-dependent repression of toxin production. Strains JIR8094, JIR8094::*codY*, and JIR8094::*ccpA* (A) and strains 630Δ*erm*, 630Δ*erm*::*fur*, 630Δ*erm*::*sigL*, and 630Δ*erm*::*sigL*(pDIA6309-*sigL*) (B) were grown for 10 h in PY or PYC. TcdA production was estimated from crude extracts by dot blot analysis using an anti-TcdA antibody. The results are representative of at least three independent experiments. (C) Effect of cysteine on *tcdA*, *tcdB*, and *tcdR* transcript levels in 630Δ*erm*::*sigL* (white boxes) or 630Δ*erm*::*sigL* complemented with pDIA6309-*sigL* (black boxes) versus the wild-type strain, 630Δ*erm*. All strains were grown for 10 h in PYC. qRT-PCR results are presented as the ratio between the amount of the mRNA (arbitrary units) of each gene normalized by the DNA Pol III gene in both 630Δ*erm*::*sigL* and 630Δ*erm*::*sigL* complemented with pDIA6309-*sigL* compared to the mRNA level in the wild-type strain. Data are the averages from at least three independent experiments, and error bars are the standard deviations from the mean values. The statistical analysis was performed by using a *t* test for all genes, with the exception of *tcdB* (Mann-Whitney test).

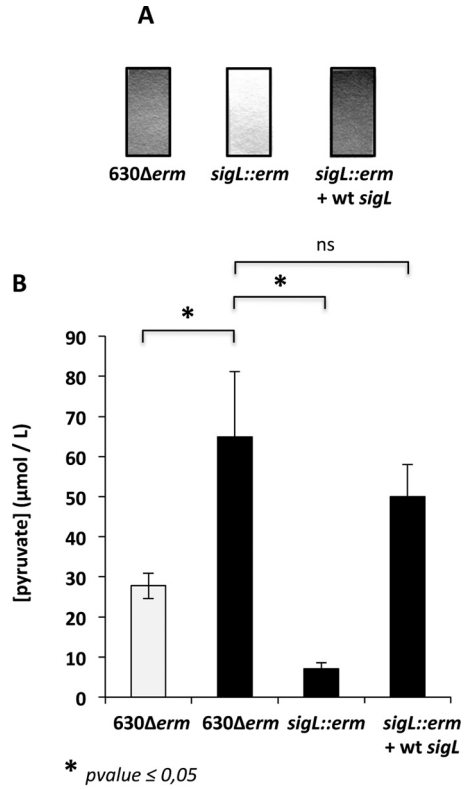

FIG 8 Effect of *sigL* inactivation on cysteine degradation and pyruvate production. (A) Detection of H_2S production in the 630Δ*erm*, 630Δ*erm*::*sigL*, and 630Δ*erm*::*sigL*(pDIA6309-*sigL*) strains grown in PYC by using lead-acetate papers. (B) Quantitative detection of pyruvate in the supernatant of strains 630Δ*erm*, 630Δ*erm*::*sigL*, and 630Δ*erm*::*sigL*(pDIA6309-*sigL*) after 10 h of growth in PY (white boxes) or PYC (black boxes). The statistical analysis was performed by using Mann-Whitney test for all genes. ns, not significant.

Involvement of pyruvate as a signal mediating toxin gene repression in response to cysteine. The accumulation of H_2S or pyruvate resulting from cysteine degradation during growth may be the signal modulating toxin production. To test this hypothesis, we added 10 mM either Na_2S or pyruvate to the PY medium when bacteria reached the stationary growth phase and harvested the cells after 1 h of exposure. The addition of pyruvate or Na_2S decreased the transcription of *tcdA*, *tcdB*, and *tcdR* (Fig. 9A). Interestingly, the effect of pyruvate was not abolished when we performed a similar experiment in the *sigL* mutant (see Fig. S4 in the supplemental material). This finding confirms that cysteine-dependent regulation of toxin production is mainly the consequence of the products of cysteine degradation. We also tested the effect of the pyruvate by-products such as formate and acetate on PaLoc gene transcription. The addition of 10 mM formate or acetate to the growing cells for 1 h did not affect the transcription of *tcdA*, *tcdB*, and *tcdR* (Fig. 9B). Thus, we concluded that pyruvate and probably sulfide are metabolic signals mediating the cysteine-dependent repression of toxin production. As the downregulation of toxin gene expression in the presence of cysteine (Fig. 2C) is more prominent than in the presence of pyruvate or sulfide alone (Fig. 9A), it is possible that the cysteine by-products could have a combined effect on toxin production.

Identification of a TCS regulating toxin gene expression in response to pyruvate. Pyruvate is a central metabolite of bacteria, and its cellular concentration is tightly controlled. In a broad range of bacteria, including *E. coli* and *Bacillus licheniformis*, pyruvate is excreted into the medium at the end of the exponential growth phase under the conditions of overflow metabolism. This compound is further taken up and metabolized (79, 80). In *E. coli*, the two-component system (TCS) YpdA-YpdB, which is also present in *B. licheniformis* (81), reacts predominantly to the presence of exogenous pyruvate and induces the expression of *yhjX*, which encodes a transporter of the major facilitator superfamily (79). The YpdA/YpdB system probably contributes to nutrient scavenging before entry into the stationary phase. In the genome of all of the *C. difficile* strains sequenced, we found a TCS (CD2602-CD2601) that is highly similar to YpdA-YpdB. Importantly, the transmembrane receptor domain of CD2602 shares 53% identity and 79% similarity with that of the histidine kinase YpdA, suggesting a common signal for these kinases. To determine whether CD2602-CD2601 is involved in the regulation of toxin gene expression in response to the level of exogenous pyruvate, we inactivated the *CD2602* gene in strain 630Δ*erm* (see Fig. S1 in the supplemental material). Then we tested the effect of pyruvate on *tcdA*, *tcdB*, and *tcdR* transcription in the *CD2602* mutant. The temporary addition of pyruvate during the growth of the *CD2602* mutant had a less pronounced effect on toxin gene transcription than it had in the wild-type strain (Fig. 9C). This result suggests that the transcriptional regulation of *tcdA*, *tcdB*, and *tcdR* in response to pyruvate availability is, at least in part, mediated by the TCS CD2602-CD2601.

Conclusion. Addition of cysteine to PY medium leads to dramatic changes in the pattern of expression of *C. difficile* genes involved in several processes, including sulfur and iron metabolism, fermentation, and the stress response. These effects on gene transcription are probably related to modifications of the metabolite pools, as we showed for the repression of toxin production by metabolic changes due to cysteine degradation and transcriptional control by cysteine through a still-uncharacterized regulator. We identified SigL as a major regulator of cysteine-dependent repression of *C. difficile* toxin production. We found that the levels of H_2S and pyruvate resulting from cysteine degradation by cysteine desulfhydrases (32) were decreased in a *sigL* mutant, which no longer repressed toxin genes in the presence of cysteine. A similar regulation of toxin production through the metabolic conversion of cysteine to sulfate and pyruvate has been observed in *B. pertussis* (21). SigL also seems to play an important role in the control of pyruvate metabolism in *Listeria monocytogenes* (82), as observed in *C. difficile* with a drop in the pyruvate concentration in the *sigL* mutant. Among the cysteine by-products produced in *C. difficile*, we demonstrated that the addition of pyruvate or H_2S to PY is sufficient to repress toxin gene expression, suggesting that pyruvate and H_2S, rather than cysteine, must be metabolic signals regulating toxin production. Interestingly, when strain 630Δ*erm* grows in the presence of cysteine, genes involved in the synthesis of pyruvate from glucose or cysteine are upregulated, while genes required for pyruvate dissimilation leading to butyrate (*buk* operon) and lactate (*ldh*) production or involved in the biosynthesis of amino acids or fatty acids from pyruvate and acetyl-CoA, respectively, are downregulated (Fig. 6). This change leads to the accumulation of pyruvate in the extracellular medium (Fig. 7B), where it is probably sensed by the membrane-associated kinase CD2602. Thus, in response to pyruvate, the response regulator CD2601 might negatively control toxin gene expression, either

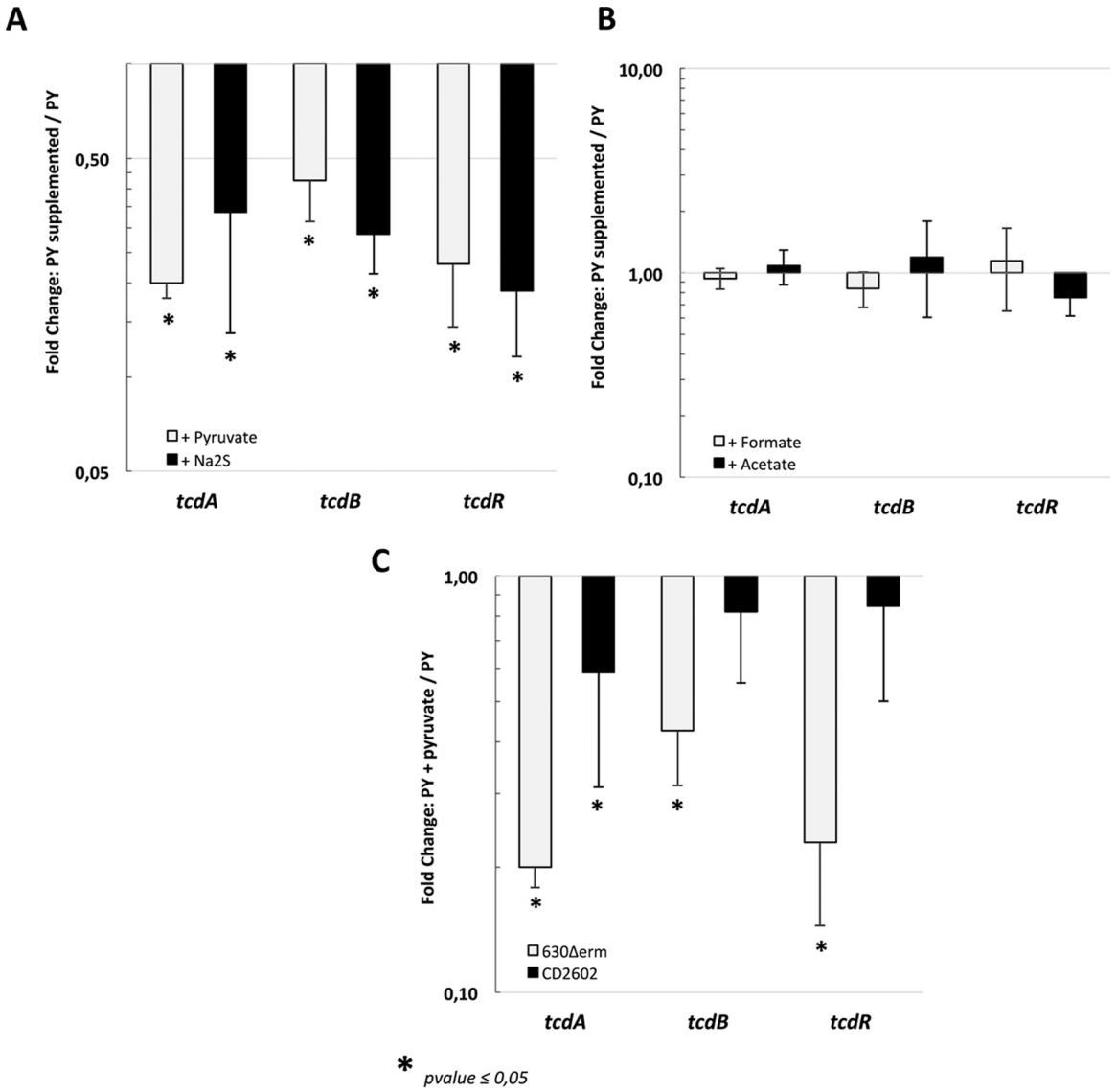

FIG 9 Effect of pyruvate and Na_2S on toxin gene expression. (A) Transcript levels of the *tcdA*, *tcdB*, and *tcdR* genes in strain 630Δ*erm* after 1 h of exposure to pyruvate (white boxes) or Na_2S (black boxes). The strain was grown in PY for 9 h, and 10 mM pyruvate or 10 mM Na_2S was then added to the medium. Cells were centrifuged 1 h later. The statistical analysis was performed by using a *t* test for all genes, with an exception for *tcdB* plus Na_2S (Mann-Whitney test). (B) Transcript levels of the *tcdA*, *tcdB*, and *tcdR* genes of strain 630Δ*erm* after 1 h of exposure to formate (white boxes) or acetate (black boxes). The strain was grown in PY for 9 h, 10 mM formate or 10 mM acetate was then added to the medium, and cells were centrifuged 1 h later. The statistical analysis was performed by using a *t* test for all genes, with the exception of *tcdB* plus acetate (Mann-Whitney test). (C) Transcript levels of the *tcdA*, *tcdB*, and *tcdR* genes of strain 630Δ*erm* (white boxes) and 630Δ*erm*::*CD2602* (black boxes) after exposure to pyruvate for 1 h, as described for panel A. qRT-PCR results are presented as the ratio between the amount of mRNA (arbitrary units) of each gene normalized by the DNA Pol III gene from bacterial cells grown in PY supplemented with one of the compounds (pyruvate, Na_2S, formate, or acetate) compared to the amount of mRNA in the untreated cells. Data are the averages from at least three independent experiments, and error bars are the standard deviations from the mean values. The statistical analysis was performed by using a *t* test for all genes, with the exception of *tcdR* plus pyruvate (Mann-Whitney test).

directly or indirectly. Conversely, butyrate, which is known to positively regulate toxin expression (12), is found at a lower concentration in the extracellular medium (see Fig. S2 in the supplemental material), which no longer stimulates toxin synthesis. Recently, it has been shown that *C. difficile* can grow in all parts of the intestinal tract of a mouse model, while toxins are only produced in the cecum and colon (83). Thus, according to the metabolites present in the small intestine and in the colon, toxin genes might be differentially expressed in the gut. Accordingly, formate and acetate (directly obtained from pyruvate) predominate in the small intestine, while the levels of propionate and butyrate are higher in the colon (84). Such a control has been described in *Salmonella enterica* serovar Typhimurium: formate acts as a diffusible signal to induce the expression of invasion genes in the small intestine, the site that is preferentially colonized by this enteropathogen, while butyrate is present at higher concentrations in the colon and represses these genes (85, 86). It is tempting to speculate that the high level of pyruvate in the small intestine represses the expression of *C. difficile* toxin genes, while butyrate mainly present in the colon induces toxin synthesis. Further bio-

chemical studies will be necessary to characterize the signal transduction pathway of the CD2602-CD2601 TCS. Thus, the ability of *C. difficile* to monitor the pyruvate level to adapt its physiology, metabolism, and virulence might be crucial to the success of a CDI.

ACKNOWLEDGMENTS

This work was supported by funding from the Institut Pasteur. M. Dancer-Thibonnier and T. Dubois are postdoctoral fellows from the PTR program funded by the Institut Pasteur (PTR256) and the French region Ile-de-France (DIM-Malinf), respectively.

We thank Philippe Bouvet for help with the CPG analysis and Roselyne Garnotel and Sophie Roulin for the intracellular amino acid content assays.

FUNDING INFORMATION

This work, including the efforts of Thomas Dubois, was funded by French Region ile de France (DIM-Malinf). This work, including the efforts of Marie Dancer-Thibonnier, was funded by Institut Pasteur (PTR 256).

REFERENCES

1. **Freeman J, Bauer MP, Baines SD, Corver J, Fawley WN, Goorhuis B, Kuijper EJ, Wilcox MH.** 2010. The changing epidemiology of Clostridium difficile infections. Clin Microbiol Rev **23:**529–549. http://dx.doi.org/10.1128/CMR.00082-09.
2. **Carter GP, Douce GR, Govind R, Howarth PM, Mackin KE, Spencer J, Buckley AM, Antunes A, Kotsanas D, Jenkin GA, Dupuy B, Rood JI, Lyras D.** 2011. The anti-sigma factor TcdC modulates hypervirulence in an epidemic BI/NAP1/027 clinical isolate of Clostridium difficile. PLoS Pathog **7:**e1002317. http://dx.doi.org/10.1371/journal.ppat.1002317.
3. **Mani N, Dupuy B.** 2001. Regulation of toxin synthesis in Clostridium difficile by an alternative RNA polymerase sigma factor. Proc Natl Acad Sci U S A **98:**5844–5849. http://dx.doi.org/10.1073/pnas.101126598.
4. **Matamouros S, England P, Dupuy B.** 2007. *Clostridium difficile* toxin expression is inhibited by the novel regulator TcdC. Mol Microbiol **64:**1274–1288. http://dx.doi.org/10.1111/j.1365-2958.2007.05739.x.
5. **Govind R, Dupuy B.** 2012. Secretion of Clostridium difficile toxins A and B requires the holin-like protein TcdE. PLoS Pathog **8:**e1002727. http://dx.doi.org/10.1371/journal.ppat.1002727.
6. **Akerlund T, Svenungsson B, Lagergren A, Burman LG.** 2006. Correlation of disease severity with fecal toxin levels in patients with *Clostridium difficile*-associated diarrhea and distribution of PCR ribotypes and toxin yields in vitro of corresponding isolates. J Clin Microbiol **44:**353–358. http://dx.doi.org/10.1128/JCM.44.2.353-358.2006.
7. **Dupuy B, Sonenshein AL.** 1998. Regulated transcription of Clostridium difficile toxin genes. Mol Microbiol **27:**107–120. http://dx.doi.org/10.1046/j.1365-2958.1998.00663.x.
8. **Karlsson S, Dupuy B, Mukherjee K, Norin E, Burman LG, Akerlund T.** 2003. Expression of Clostridium difficile toxins A and B and their sigma factor TcdD is controlled by temperature. Infect Immun **71:**1784–1793. http://dx.doi.org/10.1128/IAI.71.4.1784-1793.2003.
9. **Deneve C, Delomenie C, Barc MC, Collignon A, Janoir C.** 2008. Antibiotics involved in Clostridium difficile-associated disease increase colonization factor gene expression. J Med Microbiol **57:**732–738. http://dx.doi.org/10.1099/jmm.0.47676-0.
10. **Bouillaut L, Self WT, Sonenshein AL.** 2013. Proline-dependent regulation of Clostridium difficile Stickland metabolism. J Bacteriol **195:**844–854. http://dx.doi.org/10.1128/JB.01492-12.
11. **Karlsson S, Burman LG, Akerlund T.** 2008. Induction of toxins in Clostridium difficile is associated with dramatic changes of its metabolism. Microbiology **154:**3430–3436. http://dx.doi.org/10.1099/mic.0.2008/019778-0.
12. **Karlsson S, Lindberg A, Norin E, Burman LG, Akerlund T.** 2000. Toxins, butyric acid, and other short-chain fatty acids are coordinately expressed and down-regulated by cysteine in *Clostridium difficile*. Infect Immun **68:**5881–5888. http://dx.doi.org/10.1128/IAI.68.10.5881-5888.2000.
13. **Antunes A, Martin-Verstraete I, Dupuy B.** 2011. CcpA mediated repression of *Clostridium difficile* toxin gene expression. Mol Microbiol **79:**882–899. http://dx.doi.org/10.1111/j.1365-2958.2010.07495.x.
14. **Dineen SS, Villapakkam AC, Nordman JT, Sonenshein AL.** 2007. Repression of *Clostridium difficile* toxin gene expression by CodY. Mol Microbiol **66:**206–219. http://dx.doi.org/10.1111/j.1365-2958.2007.05906.x.
15. **Saujet L, Monot M, Dupuy B, Soutourina O, Martin-Verstraete I.** 2011. The key sigma factor of transition phase, SigH, controls sporulation, metabolism, and virulence factor expression in Clostridium difficile. J Bacteriol **193:**3186–3196. http://dx.doi.org/10.1128/JB.00272-11.
16. **Underwood S, Guan S, Vijayasubhash V, Baines SD, Graham L, Lewis RJ, Wilcox MH, Stephenson K.** 2009. Characterization of the sporulation initiation pathway of *Clostridium difficile* and its role in toxin production. J Bacteriol **191:**7296–7305. http://dx.doi.org/10.1128/JB.00882-09.
17. **Dineen SS, McBride SM, Sonenshein AL.** 2010. Integration of metabolism and virulence by *Clostridium difficile* CodY. J Bacteriol **192:**5350–5362. http://dx.doi.org/10.1128/JB.00341-10.
18. **Antunes A, Camiade E, Monot M, Courtois E, Barbut F, Sernova NV, Rodionov DA, Martin-Verstraete I, Dupuy B.** 2012. Global transcriptional control by glucose and carbon regulator CcpA in Clostridium difficile. Nucleic Acids Res **40:**10701–10718. http://dx.doi.org/10.1093/nar/gks864.
19. **Theriot CM, Koenigsknecht MJ, Carlson PE, Jr, Hatton GE, Nelson AM, Li B, Huffnagle GB, Li JZ, Young VB.** 2014. Antibiotic-induced shifts in the mouse gut microbiome and metabolome increase susceptibility to Clostridium difficile infection. Nat Commun **5:**3114. http://dx.doi.org/10.1038/ncomms4114.
20. **Andre G, Haudecoeur E, Monot M, Ohtani K, Shimizu T, Dupuy B, Martin-Verstraete I.** 2010. Global regulation of gene expression in response to cysteine availability in *Clostridium perfringens*. BMC Microbiol **10:**234. http://dx.doi.org/10.1186/1471-2180-10-234.
21. **Bogdan JA, Nazario-Larrieu J, Sarwar J, Alexander P, Blake MS.** 2001. Bordetella pertussis autoregulates pertussis toxin production through the metabolism of cysteine. Infect Immun **69:**6823–6830. http://dx.doi.org/10.1128/IAI.69.11.6823-6830.2001.
22. **Grifantini R, Bartolini E, Muzzi A, Draghi M, Frigimelica E, Berger J, Randazzo F, Grandi G.** 2002. Gene expression profile in *Neisseria meningitidis* and *Neisseria lactamica* upon host-cell contact: from basic research to vaccine development. Ann N Y Acad Sci **975:**202–216. http://dx.doi.org/10.1111/j.1749-6632.2002.tb05953.x.
23. **Hatzios SK, Bertozzi CR.** 2011. The regulation of sulfur metabolism in Mycobacterium tuberculosis. PLoS Pathog **7:**e1002036. http://dx.doi.org/10.1371/journal.ppat.1002036.
24. **Mendez J, Reimundo P, Perez-Pascual D, Navais R, Gomez E, Guijarro JA.** 2011. A novel cdsAB operon is involved in the uptake of L-cysteine and participates in the pathogenesis of Yersinia ruckeri. J Bacteriol **193:**944–951. http://dx.doi.org/10.1128/JB.01058-10.
25. **Shelver D, Rajagopal L, Harris TO, Rubens CE.** 2003. MtaR, a regulator of methionine transport, is critical for survival of group B streptococcus in vivo. J Bacteriol **185:**6592–6599. http://dx.doi.org/10.1128/JB.185.22.6592-6599.2003.
26. **Xayarath B, Marquis H, Port GC, Freitag NE.** 2009. Listeria monocytogenes CtaP is a multifunctional cysteine transport-associated protein required for bacterial pathogenesis. Mol Microbiol **74:**956–973. http://dx.doi.org/10.1111/j.1365-2958.2009.06910.x.
27. **Soutourina O, Dubrac S, Poupel O, Msadek T, Martin-Verstraete I.** 2010. The pleiotropic CymR regulator of Staphylococcus aureus plays an important role in virulence and stress response. PLoS Pathog **6:**e1000894. http://dx.doi.org/10.1371/journal.ppat.1000894.
28. **Masip L, Veeravalli K, Georgiou G.** 2006. The many faces of glutathione in bacteria. Antioxid Redox Signal **8:**753–762. http://dx.doi.org/10.1089/ars.2006.8.753.
29. **Zeller T, Klug G.** 2006. Thioredoxins in bacteria: functions in oxidative stress response and regulation of thioredoxin genes. Naturwissenschaften **93:**259–266. http://dx.doi.org/10.1007/s00114-006-0106-1.
30. **Guédon E, Martin-Verstraete I.** 2007. Cysteine metabolism and its regulation in bacteria, p 195–218. *In* Wendisch VF (ed), Amino acid biosynthesis-pathways, regulation and metabolic engineering. Springer, Berlin, Germany.
31. **Hullo MF, Auger S, Soutourina O, Barzu O, Yvon M, Danchin A, Martin-Verstraete I.** 2007. Conversion of methionine to cysteine in *Bacillus subtilis* and its regulation. J Bacteriol **189:**187–197. http://dx.doi.org/10.1128/JB.01273-06.
32. **Auger S, Gomez MP, Danchin A, Martin-Verstraete I.** 2005. The PatB protein of *Bacillus subtilis* is a C-S-lyase. Biochimie **87:**231–238. http://dx.doi.org/10.1016/j.biochi.2004.09.007.
33. **Gutierrez-Preciado A, Henkin TM, Grundy FJ, Yanofsky C, Merino E.**

2009. Biochemical features and functional implications of the RNA-based T-box regulatory mechanism. Microbiol Mol Biol Rev **73:**36–61. http://dx.doi.org/10.1128/MMBR.00026-08.

34. **Even S, Burguière P, Auger S, Soutourina O, Danchin A, Martin-Verstraete I.** 2006. Global control of cysteine metabolism by CymR in *Bacillus subtilis*. J Bacteriol **188:**2184–2197. http://dx.doi.org/10.1128/JB.188.6.2184-2197.2006.
35. **Soutourina O, Poupel O, Coppee JY, Danchin A, Msadek T, Martin-Verstraete I.** 2009. CymR, the master regulator of cysteine metabolism in Staphylococcus aureus, controls host sulfur source utilization and plays a role in biofilm formation. Mol Microbiol **73:**194–211. http://dx.doi.org/10.1111/j.1365-2958.2009.06760.x.
36. **Fagan RP, Fairweather NF.** 2011. Clostridium difficile has two parallel and essential Sec secretion systems. J Biol Chem **286:**27483–27493. http://dx.doi.org/10.1074/jbc.M111.263889.
37. **Lopez del Castillo Lozano M, Tache R, Bonnarme P, Landaud S.** 2007. Evaluation of a quantitative screening method for hydrogen sulfide production by cheese-ripening microorganisms: the first step towards L-cysteine catabolism. J Microbiol Methods **69:**70–77. http://dx.doi.org/10.1016/j.mimet.2006.12.001.
38. **Tanous C, Soutourina O, Raynal B, Hullo MF, Mervelet P, Gilles AM, Noirot P, Danchin A, England P, Martin-Verstraete I.** 2008. The CymR regulator in complex with the enzyme CysK controls cysteine metabolism in *Bacillus subtilis*. J Biol Chem **283:**35551–35560. http://dx.doi.org/10.1074/jbc.M805951200.
39. **Heap JT, Pennington OJ, Cartman ST, Carter GP, Minton NP.** 2007. The ClosTron: a universal gene knock-out system for the genus Clostridium. J Microbiol Methods **70:**452–464. http://dx.doi.org/10.1016/j.mimet.2007.05.021.
40. **Heap JT, Pennington OJ, Cartman ST, Minton NP.** 2009. A modular system for Clostridium shuttle plasmids. J Microbiol Methods **78:**79–85. http://dx.doi.org/10.1016/j.mimet.2009.05.004.
41. **Livak KJ, Schmittgen TD.** 2001. Analysis of relative gene expression data using real-time quantitative PCR and the $2^{-\Delta\Delta CT}$ method. Methods **25:**402–408. http://dx.doi.org/10.1006/meth.2001.1262.
42. **Breitling R, Armengaud P, Amtmann A, Herzyk P.** 2004. Rank products: a simple, yet powerful, new method to detect differentially regulated genes in replicated microarray experiments. FEBS Lett **573:**83–92. http://dx.doi.org/10.1016/j.febslet.2004.07.055.
43. **Smyth GK, Speed T.** 2003. Normalization of cDNA microarray data. Methods **31:**265–273. http://dx.doi.org/10.1016/S1046-2023(03)00155-5.
44. **Benjamini Y, Hochberg Y.** 1995. Controlling the false discovery rate: a practical and powerful approach to multiple testing. J R Statist Soc Ser **57:**289–300.
45. **Sebaihia M, Wren BW, Mullany P, Fairweather NF, Minton N, Stabler R, Thomson NR, Roberts AP, Cerdeno-Tarraga AM, Wang H, Holden MT, Wright A, Churcher C, Quail MA, Baker S, Bason N, Brooks K, Chillingworth T, Cronin A, Davis P, Dowd L, Fraser A, Feltwell T, Hance Z, Holroyd S, Jagels K, Moule S, Mungall K, Price C, Rabbinowitsch E, Sharp S, Simmonds M, Stevens K, Unwin L, Whithead S, Dupuy B, Dougan G, Barrell B, Parkhill J.** 2006. The multidrug-resistant human pathogen *Clostridium difficile* has a highly mobile, mosaic genome. Nat Genet **38:**779–786. http://dx.doi.org/10.1038/ng1830.
46. **Mehta PK, Christen P.** 2000. The molecular evolution of pyridoxal-5′-phosphate-dependent enzymes. Adv Enzymol Relat Areas Mol Biol **74:**129–184.
47. **Andre G, Even S, Putzer H, Burguiere P, Croux C, Danchin A, Martin-Verstraete I, Soutourina O.** 2008. S-box and T-box riboswitches and antisense RNA control a sulfur metabolic operon of Clostridium acetobutylicum. Nucleic Acids Res **36:**5955–5969. http://dx.doi.org/10.1093/nar/gkn601.
48. **Manukhov IV, Mamaeva DV, Rastorguev SM, Faleev NG, Morozova EA, Demidkina TV, Zavilgelsky GB.** 2005. A gene encoding L-methionine gamma-lyase is present in Enterobacteriaceae family genomes: identification and characterization of Citrobacter freundii L-methionine gamma-lyase. J Bacteriol **187:**3889–3893. http://dx.doi.org/10.1128/JB.187.11.3889-3893.2005.
49. **Dias B, Weimer B.** 1998. Purification and characterization of L-methionine gamma-lyase from *Brevibacterium linens* BL2. Appl Environ Microbiol **64:**3327–3331.
50. **Ali V, Nozaki T.** 2007. Current therapeutics, their problems, and sulfur-containing-amino-acid metabolism as a novel target against infections by "amitochondriate" protozoan parasites. Clin Microbiol Rev **20:**164–187. http://dx.doi.org/10.1128/CMR.00019-06.
51. **Dembek M, Barquist L, Boinett CJ, Cain AK, Mayho M, Lawley TD, Fairweather NF, Fagan RP.** 2015. High-throughput analysis of gene essentiality and sporulation in Clostridium difficile. mBio **6:**e02383–14. http://dx.doi.org/10.1128/mBio.02383-14.
52. **Boudry P, Gracia C, Monot M, Caillet J, Saujet L, Hajnsdorf E, Dupuy B, Martin-Verstraete I, Soutourina O.** 2014. Pleiotropic role of the RNA chaperone protein Hfq in the human pathogen Clostridium difficile. J Bacteriol **196:**3234–3248. http://dx.doi.org/10.1128/JB.01923-14.
53. **Neumann-Schaal M, Hofmann JD, Will SE, Schomburg D.** 2015. Time-resolved amino acid uptake of Clostridium difficile 630Deltaerm and concomitant fermentation product and toxin formation. BMC Microbiol **15:**281. http://dx.doi.org/10.1186/s12866-015-0614-2.
54. **Hullo MF, Auger S, Dassa E, Danchin A, Martin-Verstraete I.** 2004. The *metNPQ* operon of *Bacillus subtilis* encodes an ABC permease transporting methionine sulfoxide, D- and L-methionine. Res Microbiol **155:**80–86. http://dx.doi.org/10.1016/j.resmic.2003.11.008.
55. **Rodionov DA, Vitreschak AG, Mironov AA, Gelfand MS.** 2004. Comparative genomics of the methionine metabolism in Gram-positive bacteria: a variety of regulatory systems. Nucleic Acids Res **32:**3340–3353. http://dx.doi.org/10.1093/nar/gkh659.
56. **Soutourina OA, Monot M, Boudry P, Saujet L, Pichon C, Sismeiro O, Semenova E, Severinov K, Le Bouguenec C, Coppee JY, Dupuy B, Martin-Verstraete I.** 2013. Genome-wide identification of regulatory RNAs in the human pathogen Clostridium difficile. PLoS Genet **9:**e1003493. http://dx.doi.org/10.1371/journal.pgen.1003493.
57. **Burguiere P, Auger S, Hullo MF, Danchin A, Martin-Verstraete I.** 2004. Three different systems participate in L-cystine uptake in *Bacillus subtilis*. J Bacteriol **186:**4875–4884. http://dx.doi.org/10.1128/JB.186.15.4875-4884.2004.
58. **Awano N, Wada M, Mori H, Nakamori S, Takagi H.** 2005. Identification and functional analysis of Escherichia coli cysteine desulfhydrases. Appl Environ Microbiol **71:**4149–4152. http://dx.doi.org/10.1128/AEM.71.7.4149-4152.2005.
59. **Hindson VJ.** 2003. Serine acetyltransferase of Escherichia coli: substrate specificity and feedback control by cysteine. Biochem J **375:**745–752. http://dx.doi.org/10.1042/bj20030429.
60. **Harris CL.** 1981. Cysteine and growth inhibition of *Escherichia coli*: threonine deaminase as the target enzyme. J Bacteriol **145:**1031–1035.
61. **Lee JW, Helmann JD.** 2007. Functional specialization within the Fur family of metalloregulators. Biometals **20:**485–499. http://dx.doi.org/10.1007/s10534-006-9070-7.
62. **Vasileva D, Janssen H, Honicke D, Ehrenreich A, Bahl H.** 2012. Effect of iron limitation and fur gene inactivation on the transcriptional profile of the strict anaerobe Clostridium acetobutylicum. Microbiology **158:**1918–1929. http://dx.doi.org/10.1099/mic.0.056978-0.
63. **Ollinger J, Song KB, Antelmann H, Hecker M, Helmann JD.** 2006. Role of the Fur regulon in iron transport in Bacillus subtilis. J Bacteriol **188:**3664–3673. http://dx.doi.org/10.1128/JB.188.10.3664-3673.2006.
64. **Ho TD, Ellermeier CD.** 2015. Ferric uptake regulator Fur control of putative iron acquisition systems in Clostridium difficile. J Bacteriol **197:**2930–2940. http://dx.doi.org/10.1128/JB.00098-15.
65. **Torres VJ, Attia AS, Mason WJ, Hood MI, Corbin BD, Beasley FC, Anderson KL, Stauff DL, McDonald WH, Zimmerman LJ, Friedman DB, Heinrichs DE, Dunman PM, Skaar EP.** 2010. Staphylococcus aureus Fur regulates the expression of virulence factors that contribute to the pathogenesis of pneumonia. Infect Immun **78:**1618–1628. http://dx.doi.org/10.1128/IAI.01423-09.
66. **Nielsen AH, Hvitved-Jacobsen T, Vollertsen J.** 2008. Effects of pH and iron concentrations on sulfide precipitation in wastewater collection systems. Water Environ Res **80:**380–384. http://dx.doi.org/10.2175/106143007X221328.
67. **Jackson S, Calos M, Myers A, Self WT.** 2006. Analysis of proline reduction in the nosocomial pathogen Clostridium difficile. J Bacteriol **188:**8487–8495. http://dx.doi.org/10.1128/JB.01370-06.
68. **Kim SH, Schneider BL, Reitzer L.** 2010. Genetics and regulation of the major enzymes of alanine synthesis in Escherichia coli. J Bacteriol **192:**5304–5311. http://dx.doi.org/10.1128/JB.00738-10.
69. **Vitreschak AG, Mironov AA, Lyubetsky VA, Gelfand MS.** 2008. Comparative genomic analysis of T-box regulatory systems in bacteria. RNA **14:**717–735. http://dx.doi.org/10.1261/rna.819308.
70. **Brinsmade SR, Kleijn RJ, Sauer U, Sonenshein AL.** 2010. Regulation

of CodY activity through modulation of intracellular branched-chain amino acid pools. J Bacteriol **192:**6357–6368. http://dx.doi.org/10.1128/JB.00937-10.

71. **Fonknechten N, Chaussonnerie S, Tricot S, Lajus A, Andreesen JR, Perchat N, Pelletier E, Gouyvenoux M, Barbe V, Salanoubat M, Le Paslier D, Weissenbach J, Cohen GN, Kreimeyer A.** 2010. Clostridium sticklandii, a specialist in amino acid degradation: revisiting its metabolism through its genome sequence. BMC Genomics **11:**555. http://dx.doi.org/10.1186/1471-2164-11-555.
72. **Troxell B, Hassan HM.** 2013. Transcriptional regulation by ferric uptake regulator (Fur) in pathogenic bacteria. Front Cell Infect Microbiol **3:**59. http://dx.doi.org/10.3389/fcimb.2013.00059.
73. **Dalet K, Briand C, Cenatiempo Y, Hechard Y.** 2000. The rpoN gene of Enterococcus faecalis directs sensitivity to subclass IIa bacteriocins. Curr Microbiol **41:**441–443. http://dx.doi.org/10.1007/s002840010164.
74. **Iyer VS, Hancock LE.** 2012. Deletion of sigma(54) (rpoN) alters the rate of autolysis and biofilm formation in Enterococcus faecalis. J Bacteriol **194:**368–375. http://dx.doi.org/10.1128/JB.06046-11.
75. **Mattila M, Somervuo P, Rattei T, Korkeala H, Stephan R, Tasara T.** 2012. Phenotypic and transcriptomic analyses of sigma L-dependent characteristics in Listeria monocytogenes EGD-e. Food Microbiol **32:**152–164. http://dx.doi.org/10.1016/j.fm.2012.05.005.
76. **Okada Y, Okada N, Makino S, Asakura H, Yamamoto S, Igimi S.** 2006. The sigma factor RpoN (sigma54) is involved in osmotolerance in Listeria monocytogenes. FEMS Microbiol Lett **263:**54–60. http://dx.doi.org/10.1111/j.1574-6968.2006.00405.x.
77. **Saldias MS, Lamothe J, Wu R, Valvano MA.** 2008. Burkholderia cenocepacia requires the RpoN sigma factor for biofilm formation and intracellular trafficking within macrophages. Infect Immun **76:**1059–1067. http://dx.doi.org/10.1128/IAI.01167-07.
78. **Francke C, Groot Kormelink T, Hagemeijer Y, Overmars L, Sluijter V, Moezelaar R, Siezen RJ.** 2011. Comparative analyses imply that the enigmatic sigma factor 54 is a central controller of the bacterial exterior. BMC Genomics **12:**385. http://dx.doi.org/10.1186/1471-2164-12-385.
79. **Fried L, Behr S, Jung K.** 2013. Identification of a target gene and activating stimulus for the YpdA/YpdB histidine kinase/response regulator system in Escherichia coli. J Bacteriol **195:**807–815. http://dx.doi.org/10.1128/JB.02051-12.
80. **Paczia N, Nilgen A, Lehmann T, Gatgens J, Wiechert W, Noack S.** 2012. Extensive exometabolome analysis reveals extended overflow metabolism in various microorganisms. Microb Cell Fact **11:**122. http://dx.doi.org/10.1186/1475-2859-11-122.
81. **Yangtse W, Zhou Y, Lei Y, Qiu Y, Wei X, Ji Z, Qi G, Yong Y, Chen L, Chen S.** 2012. Genome sequence of Bacillus licheniformis WX-02. J Bacteriol **194:**3561–3562. http://dx.doi.org/10.1128/JB.00572-12.
82. **Arous S, Buchrieser C, Folio P, Glaser P, Namane A, Hebraud M, Hechard Y.** 2004. Global analysis of gene expression in an rpoN mutant of Listeria monocytogenes. Microbiology **150:**1581–1590. http://dx.doi.org/10.1099/mic.0.26860-0.
83. **Koenigsknecht MJ, Theriot CM, Bergin IL, Schumacher CA, Schloss PD, Young VB.** 2015. Dynamics and establishment of Clostridium difficile infection in the murine gastrointestinal tract. Infect Immun **83:**934–941. http://dx.doi.org/10.1128/IAI.02768-14.
84. **Keeney KM, Finlay BB.** 2011. Enteric pathogen exploitation of the microbiota-generated nutrient environment of the gut. Curr Opin Microbiol **14:**92–98. http://dx.doi.org/10.1016/j.mib.2010.12.012.
85. **Gantois I, Ducatelle R, Pasmans F, Haesebrouck F, Hautefort I, Thompson A, Hinton JC, Van Immerseel F.** 2006. Butyrate specifically down-regulates Salmonella pathogenicity island 1 gene expression. Appl Environ Microbiol **72:**946–949. http://dx.doi.org/10.1128/AEM.72.1.946-949.2006.
86. **Huang Y, Suyemoto M, Garner CD, Cicconi KM, Altier C.** 2008. Formate acts as a diffusible signal to induce Salmonella invasion. J Bacteriol **190:**4233–4241. http://dx.doi.org/10.1128/JB.00205-08.
87. **Hussain HA, Roberts AP, Mullany P.** 2005. Generation of an erythromycin-sensitive derivative of Clostridium difficile strain 630 (630Deltaerm) and demonstration that the conjugative transposon Tn916DeltaE enters the genome of this strain at multiple sites. J Med Microbiol **54:**137–141. http://dx.doi.org/10.1099/jmm.0.45790-0.
88. **O'Connor JR, Lyras D, Farrow KA, Adams V, Powell DR, Hinds J, Cheung JK, Rood JI.** 2006. Construction and analysis of chromosomal *Clostridium difficile* mutants. Mol Microbiol **61:**1335–1351. http://dx.doi.org/10.1111/j.1365-2958.2006.05315.x.